


May 2017

A Novel Link Between the Chemotaxis and Biofilm Dispersion Systems of *Pseudomonas Aeruginosa*

Jesse Michael Reinhardt
University of Wisconsin-Milwaukee

Follow this and additional works at: <https://dc.uwm.edu/etd>

 Part of the [Microbiology Commons](#), and the [Molecular Biology Commons](#)

Recommended Citation

Reinhardt, Jesse Michael, "A Novel Link Between the Chemotaxis and Biofilm Dispersion Systems of *Pseudomonas Aeruginosa*" (2017). *Theses and Dissertations*. 1533.
<https://dc.uwm.edu/etd/1533>

This Dissertation is brought to you for free and open access by UWM Digital Commons. It has been accepted for inclusion in Theses and Dissertations by an authorized administrator of UWM Digital Commons. For more information, please contact open-access@uwm.edu.

A NOVEL LINK BETWEEN THE CHEMOTAXIS AND BIOFILM
DISPERSION SYSTEMS OF *PSEUDOMONAS AERUGINOSA*

by

Jesse Reinhardt

A Dissertation Submitted in
Partial Fulfillment of the
Requirements for the Degree of

Doctor of Philosophy
in Biological Sciences

at

The University of Wisconsin-Milwaukee

May 2017

ABSTRACT

A NOVEL LINK BETWEEN THE CHEMOTAXIS AND BIOFILM DISPERSION SYSTEMS OF *PSEUDOMONAS AERUGINOSA*

by

Jesse M. Reinhardt

The University of Wisconsin-Milwaukee, 2017
Under the Supervision of Professor Sonia L. Bardy

Bacterial chemotaxis is the movement of a cell towards an attractant or away from a repellent. This controlled movement is possible due to the chemotaxis system, which is typically made up of several proteins that collectively sense the stimuli and transduce the signal within the cell to mediate a motility response. The chemotaxis proteins of *Pseudomonas aeruginosa* are encoded in two clusters, which are located at different regions of the chromosome: *che I* and *che V*. These gene clusters are known to control chemotaxis via swimming, or flagellar-based, motility. When expressed, these chemotaxis proteins associate with each other to form tight clusters that are composed of thousands of copies of each protein. These clusters localize to the flagellated pole in young cells and show bi-polar localization in older cells. Within cluster *che I* are genes encoding two Par-like proteins: ParC and ParP. Both Par-like proteins are needed for wild type swimming motility, yet ParP appears to have a more important role as its loss results in a greater swimming defect. Cluster formation of the chemotaxis histidine kinase CheA was reduced by 50% in the absence of either Par-like protein, thus demonstrating a potential mechanism behind the reduced swimming motility. However, the equivalent reduction in foci formation does not explain the larger defect resulting from the absence of ParP. ParC has a predicted ATPase domain and mutation of the ATP binding site resulted in a dominant negative

swimming phenotype when expressed *in trans*. ParP has a CheW-like domain and overexpression of CheW can partially restore swimming motility to a *parP* mutant. Bacterial two-hybrid results showed that the Par-like proteins interact with each other and the chemotaxis system, and that ParP interacts with DipA, a phosphodiesterase which degrades cyclic-di-GMP and is important for biofilm dispersion and chemotaxis. Deletion of *dipA* resulted in a similar defect in swimming motility as the *parP* mutant. Surface flagellin levels were slightly increased in both the *parP* and *dipA* mutants, although it is not known if this was due to increased flagellation or longer flagella. Fluorescence microscopy results showed that ParP has an interdependence in polar cluster formation with both CheA and DipA. CheA cluster formation is dependent on ParC. Due to the direct interactions and interdependence of cluster formation of ParP and DipA, and the fact that *parP* and *dipA* mutants have similar defects in swimming motility and increases in surface flagellin levels, further investigation into the role of ParP in biofilm dispersion is warranted.

TABLE OF CONTENTS

	Page
List of Figures	vi
List of Tables	viii
Acknowledgements	ix
Chapter One: Introduction	1
1.1 Bacterial chemotaxis	2
1.1.1 Methyl-accepting chemotaxis proteins.....	4
1.1.2 Cytoplasmic chemotaxis proteins.....	9
1.2 Chemotaxis protein cluster formation, stoichiometry, and localization patterns.....	12
1.2.1 Partitioning systems	15
1.2.2 Par-like systems.....	16
1.3 <i>Pseudomonas aeruginosa</i>	19
1.3.1 Chemotaxis in <i>Pseudomonas aeruginosa</i>	20
1.4 The second messenger c-di-GMP	22
1.4.1 C-di-GMP and its impact on chemotaxis	24
1.5 Biofilm dispersion.....	26
1.6 Concluding remarks	27
Chapter Two: Materials and Methods	28
2.1 Strains, plasmids, growth conditions and media used	29
2.2 Generation of deletion mutants and expression strains.....	33
2.3 Site-directed mutagenesis	34
2.4 Growth curves	37
2.4 Bacterial two-hybrid analysis	37
2.5 SDS-PAGE and western blot.....	38
2.6 Swimming assay	38
2.7 Flagellin preparation assay	38

2.8 Fluorescence microscopy	39
2.9 Protein alignment	40
Chapter Three: Results	41
3.1 Par-like proteins are required for optimal chemotaxis in <i>Pseudomonas aeruginosa</i>	42
3.2 Chemotaxis protein localization is dependent on the Par-like proteins	45
3.3 ParP _{Pa} has a CheW-like domain.....	46
3.4 DipA interacts with ParP _{Pa} and affects swimming motility and surface flagellin levels.....	51
3.5 DipA, ParP _{Pa} and CheA polar localization is interdependent	57
3.6 ParC has a conserved ATPase domain which may be important for swimming motility ...	63
Chapter Four: Discussion	67
References	77
Curriculum Vitae	87

LIST OF FIGURES

	Page
Figure 1.1 – The chemotaxis system of <i>E. coli</i>	3
Figure 1.2 – The structure of a methyl-accepting chemotaxis protein from <i>E. coli</i>	8
Figure 3.1 – Par-like proteins are encoded within chemotaxis gene cluster I (<i>che I</i>) and are required for optimal swimming motility.....	43
Figure 3.2 – <i>parC_{Pa}</i> and <i>parP_{Pa}</i> mutants do not have a defect in their growth rate	44
Figure 3.3 – The Par-like proteins affect chemotaxis protein localization	47
Figure 3.4 – CheA-mTq is functional and present at higher levels in the <i>par</i> -like mutants	48
Figure 3.5 – CheW may have functional redundancy to the CheW-like domain of ParP	49
Figure 3.6 – Induction of His-ParP _{Pa} and His-CheW results in expression.....	50
Figure 3.7 – DipA interacts directly with ParP _{Pa} , as demonstrated by a bacterial two-hybrid assay	53
Figure 3.8 – Deletion of DipA results in a similar reduction of swimming motility as seen in $\Delta parP$	54
Figure 3.9 – Deletion of <i>parP</i> and <i>dipA</i> increases surface flagellin levels	56
Figure 3.10 – DipA is not required for CheA foci formation or localization	58
Figure 3.11 – ParP foci formation is dependent on DipA and CheA.....	59

Figure 3.12 – DipA foci formation is dependent on ParP and CheA.....	60
Figure 3.13 – Fluorescent fusion proteins Yfp-ParP and DipA-Yfp are functional	61
Figure 3.14 – Model showing the dependence on foci formation between the Par-like proteins and the chemotaxis and biofilm dispersion systems of <i>P. aeruginosa</i>	62
Figure 3.15 – Alignment of the amino acid sequences of ParA type Ia, Ib, and II proteins along with ParC _{Pa} for comparison	64
Figure 3.16 – Alignment of the amino acid sequences of ParC _{Pa} , ParC _{Vc} , and PpfA	65
Figure 3.17 – Mutation of the proposed ATP binding site has a dominant negative effect on swimming motility compared with wild type ParC	66
Figure 4.1 – Model showing B2H interactions linking the Par-like proteins with the chemotaxis and biofilm dispersion systems of <i>P. aeruginosa</i>	75

LIST OF TABLES

	Page
Table 2.1 Plasmids used in this study	30
Table 2.2 Strains used in this study	32
Table 2.3 Primers used in this study	35

ACKNOWLEDGEMENTS

I would like to thank Dr. Bardy for accepting me as a graduate student in her lab. She not only played a critical role in my overall development as a scientist, but she also fostered my growth in communication and critical thinking. These skills will serve me well in my future job positions and in my personal life – the ability to think for oneself and question things is priceless in this world. I appreciate the times that Dr. Bardy was there for me, starting when I first visited the UWM campus in March of 2011, throughout my time here working on experiments and performing research, and helping me get my thesis proposal and final thesis written – I can see that on her end it took a lot of dedication. The experience that I have had here at UWM was life-changing and I could not have asked for a better outcome.

It was wonderful working with lab mates such as Vibhuti Jansari, Laura Ketelboeter, Swati Sharma, and the various undergraduate students that came and left. I especially want to thank Vibhuti for the support we have shared over the years in getting through different milestones such as the preliminary exams and thesis writing or through small steps such as certain experiments that didn't work so well for one of us.

I want to acknowledge the Dey, Prasad, Yang, McBride and Wimpee labs and their members for their support when I needed help to keep my experiments going. I would like to thank my committee members Dr. Forst, Dr. McBride, Dr. Wimpee and Dr. Yang for their advice on new directions to take my projects and ideas for new experiments. During my first semester, I felt very welcomed by the McBride and Saffarini labs when we had a Thanksgiving lunch together. I also had the privilege to go to an early Thanksgiving dinner at Dr. Yang's house, where I got to spend time with his lab members such as Xiaochen and Liwei. On several

occasions, Dr. Bardy and her husband Graham graciously hosted myself and her other lab members for get-togethers at her house.

My family was also instrumental in my success at UWM. Without the support of my parents and grandparents, I may not have been able to even go to college for my undergraduate degree. Even after my undergraduate studies and while I was in graduate school, my family was there for me when I needed them.

My time at UWM was filled with many successes and failures. Initially, I struggled with getting traction with my experiments and I had trouble making new discoveries as a competing lab had scooped my work. In the end, I did gain traction in my work and have made new discoveries. Lastly, I want to give special acknowledgement to my family and Vibhuti for their great and undying support during these times.

Chapter One

Introduction

1.1 Bacterial chemotaxis

Bacterial chemotaxis is mediated by a two-component chemosensory system wherein a motile bacterium senses chemoeffectors in its environment and responds by moving towards favorable or away from unfavorable conditions. These chemoeffectors, or ligands, are sensed by chemoreceptor proteins that function to transduce signals across the cytoplasmic membrane to chemotaxis proteins, which in turn generate a response. In *Escherichia coli*, these proteins form tight clusters that are composed of thousands of copies of each protein (1).

Two-component signal transduction systems (TCS) are comprised of a histidine kinase and a cognate response regulator and are commonly used sensory pathways in prokaryotes (2). These systems allow bacteria to sense environmental signals such as nutrients, oxygen levels, pH and osmolarity. Most histidine kinases in two component systems have an N-terminal domain which spans the cytoplasmic membrane twice – the periplasmic region of these proteins is where signals can be sensed. The remaining C-terminal portion of the protein has histidine kinase activity. When activated, the histidine kinase phosphorylates itself and transfers that phosphate group to the cognate response regulator. The activated and phosphorylated response regulator then causes cellular changes such as alteration of gene expression, motility or receptor adaptation (2).

In contrast to the classical two-component histidine kinase, the chemotaxis histidine kinase (CheA) lacks transmembrane (TM) and periplasmic domains, localizes in the cytoplasm and interacts with TM chemoreceptors (2). It is these TM chemoreceptors that sense the environmental stimuli and the output of this system is altered motility and adaptation, resulting in chemotaxis. The chemotaxis system of *E. coli* is the most well-studied and will be described here (Figure 1.1).

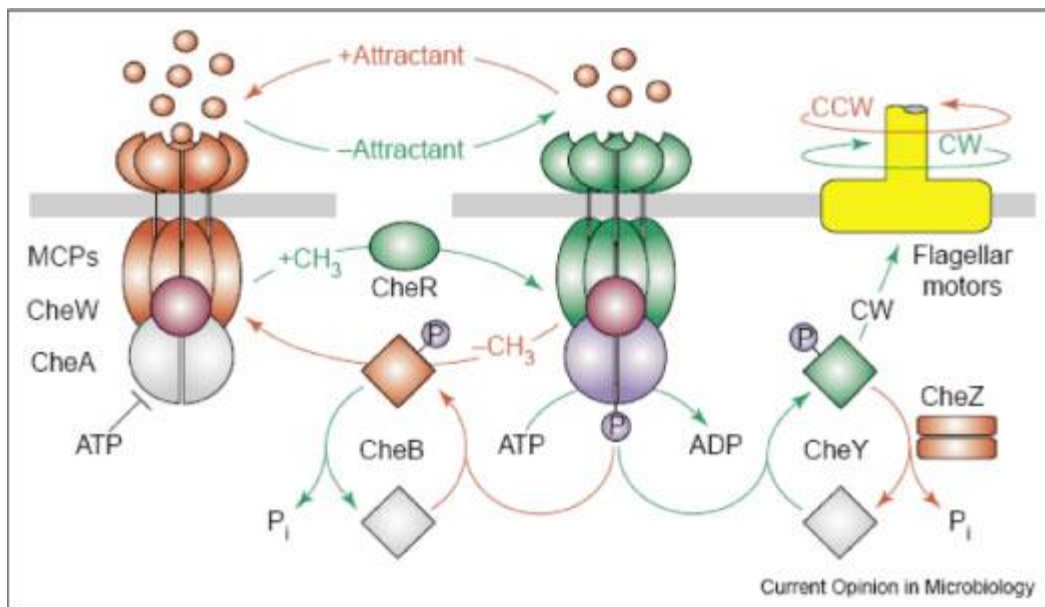


Figure 1.1 – The chemotaxis system of *E. coli*. Adapted from (3).

1.1.1 Methyl-accepting chemotaxis proteins

Methyl-accepting chemotaxis proteins (MCPs) are chemoreceptors which sense environmental stimuli. Most bacterial species have multiple MCPs which allow them to sense a variety of signals such as amino acids, oxygen and other organic carbon sources such as succinate or fumarate (4). For example, *E. coli* has 4 MCPs whereas *Pseudomonas aeruginosa* has 26 predicted MCPs. The cytoplasmic domains of these MCPs are highly conserved and are often used in identifying their genes (5). However, the periplasmic domain is variable within different MCPs and different bacterial species, which is likely because various ligands are bound in this domain (2). MCPs have been observed to localize in the inner membrane and in the cytoplasm (5-8). In *E. coli*, the overall structure of an MCP is largely α -helical coiled-coil (9). TM MCPs form homodimers that spontaneously group into trimers of dimers. These trimers of dimers can then form higher order clusters of large signaling complexes (10, 11). Within the MCP homodimer, each monomer has three main functional units that have distinct features and functions – ligand binding, input-output control and kinase control (12). The N-terminus of each MCP monomer is in the cytoplasm and then continues into the inner membrane and the periplasm as a single α -helix (Figure 1.2). Within the periplasm, each monomer forms three additional α -helices that are linked together and the last helix continues back into the inner membrane and the cytoplasm (Figure 1.2). In the periplasm, the four TM helices, two from each monomer, associate together to form the ligand binding domain, which consists of a four-helix bundle and is where signaling is initiated upon ligand binding (12). The last helix of each MCP monomer in the ligand binding domain continues into the inner membrane where, together with the first TM helix following the N-terminus, they form another four-helix bundle within the homodimer that makes up the TM domain (13). The TM domain conveys signals across the inner

membrane and into the cytoplasm via conformational changes through the second transmembrane helix of each monomer (14). This second transmembrane helix continues into the cytoplasm to form the input-output control unit which consists of a 5-residue control cable (Figure 1.2). This cable acts as the linker that translates signals from the TM helices to the HAMP domain via conformational changes. After the control cable is the 50-residue HAMP domain (Histidine kinases, Adenylyl cyclases, Methyl-accepting proteins and Phosphatases) (15). When activated by ligand binding, the TM domain may make piston motions which alter the control cable helicity and influence HAMP domain stability (16). Since TM proteins are difficult to study due to their hydrophobicity, several models have been proposed to explain exactly how the HAMP domain takes signals from the TM domain and transmits them to the cytoplasm. Although there is no unifying mechanism for how this process works, it is generally thought that conformational changes in the helices of the HAMP domain allow signal transduction (13). Following the HAMP domain are two long helices within each monomer that are folded onto each other and make up the kinase control unit (Figure 1.2). The first part of this unit is called the adaptation region and this is where methylation of the MCP takes place and results in adaptation of the receptor to the concentrations of ligand in the environment (12). The adaptation region of each monomer can have four or more glutamate or glutamine residues. The glutamate residues can be modified by methylation or demethylation to produce adaptation whereas the glutamine residues are “inactive” until they are deamidated to form glutamate. These glutamine residues are probably present to ensure that when an MCP is inserted in the cytoplasmic membrane it is in a neutral signaling state (2). Methylation of the glutamate residue has an overall effect of neutralizing the negative charge of the side chain. This would favor closer helical packing and an MCP conformation that favors CheA activation (10). Following the

adaptation region is the flexible bundle, which has a conserved glycine hinge consisting of six glycine residues within each monomer that allows its long axis to bend 10° (17). This region is crucial for proper kinase control as substituting the glycine residues for larger residues results in the receptor being locked in a kinase-on or -off conformation (17). After the flexible bundle is the signaling region, which is comprised of a hairpin tip - a short sequence of amino acids that links two α -helices of an MCP monomer (12). The hairpin tip is highly conserved and is therefore a defining sequence motif of MCPs. The tip functions by interacting with CheW (adaptor) and CheA (histidine kinase) to mediate chemotactic responses (9, 18). Within this signaling region are also trimer contact sites that allow the MCP homodimers to interact with other dimers to form trimers of dimers (12, 16, 19). After the last helix of each MCP monomer is the flexible arm, which is ~30 residues long and protrudes from the MCP body. The flexible arm helps to tether the methylation proteins to the MCP (10). This arm, as the name suggests, is flexible and allows the methylation proteins access to the adaptation regions of nearby MCPs so that they can perform their function. However, the flexible arm itself does not directly bind the methylation proteins, but immediately after the arm on the C-terminal end of the *E. coli* receptors Tar and Tsr is a conserved pentapeptide sequence (NWET/SF) that binds to the methylation proteins CheB (methyltransferase) and CheR (methyltransferase) and keeps them in close proximity to the adaptation region of the MCP (Figure 1.2) (20, 21). Deletion of this conserved sequence from the C-terminal end of the MCP results in much less efficient methylation and demethylation but histidine kinase activation and MCP signal transduction are otherwise unaffected (21). In *E. coli*, MCPs may be present at high or low abundance and there is an approximate 10-fold difference in cellular levels between these MCP types (14). Lower abundance MCPs such as Trg and Tap lack the NWET/SF motif and therefore rely on the presence of the higher abundance

MCPs Tar and Tsr for adaptation to their ligand (14). Large clusters of both high and low abundance MCPs allow lower abundance ones to share tethered methylation proteins from other MCP dimers (10).

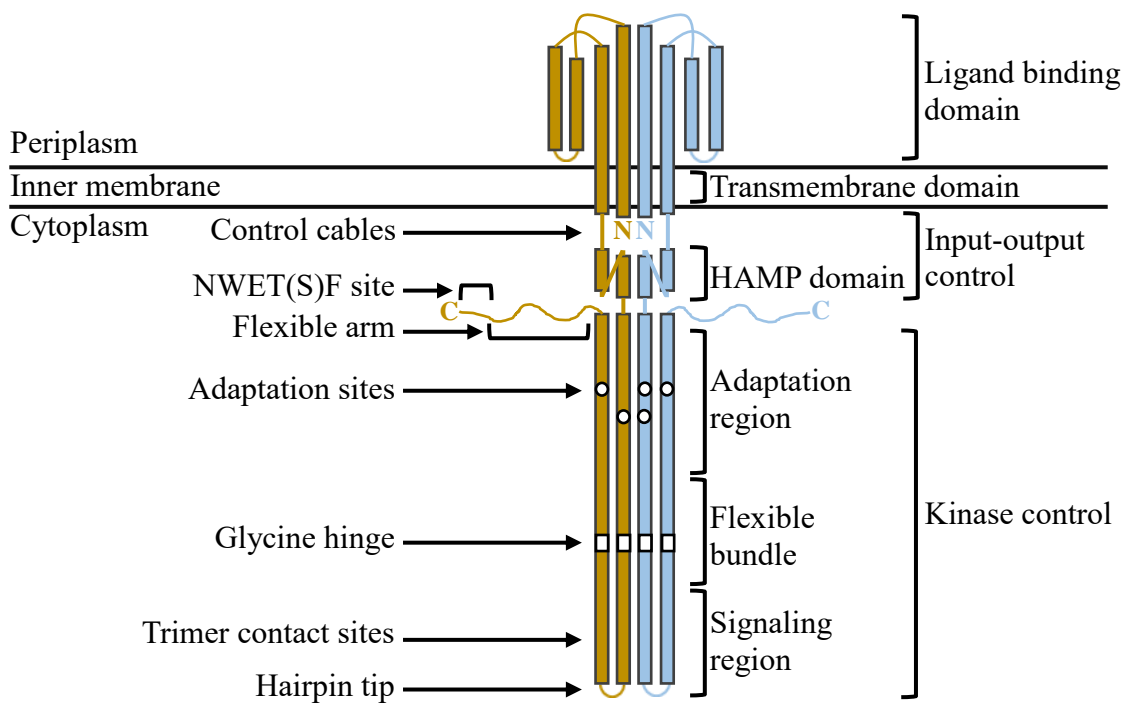


Figure 1.2 - The structure of a methyl-accepting chemotaxis protein from *E. coli*. The rectangles indicate α -helices, white circles indicate adaptation sites where methylation takes place, and white boxes indicate the glycine hinges of each MCP monomer. The N-terminus is denoted by “N” and the C-terminus is denoted by “C”. Modified from (12).

1.1.2 Cytoplasmic chemotaxis proteins

Signals are transferred from MCPs to the cytoplasmic chemotaxis proteins (Figure 1.1). As mentioned earlier, CheA and CheW interact with the signaling domain of the MCP. CheW is an adaptor protein which acts as a monomeric scaffold for the MCP and CheA to form a stable signaling complex and is essential for signal transduction (2, 22). Aside from this role as a scaffolding protein, CheW has no known catalytic activity. However, in many bacteria, the number of encoded CheW proteins do not correspond to the number of CheA proteins, which suggests that there is not always one CheW made for each CheA (2).

CheA is a histidine kinase that plays a crucial role in chemotaxis wherein it receives signals from MCPs and in turn mediates responses by phosphorylating the response regulators CheB (methyl-erastase) and CheY. In *E. coli*, CheA has five domains which are used for: trans-autophosphorylation (P1), phosphoacceptor binding (P2), dimerization (P3), ATP binding (P4) and chemoreceptor control (P5) (22). CheA exists as a homodimer and, upon MCP activation, catalyzes the reversible trans-autophosphorylation of a gamma phosphate group from ATP bound to one monomer onto a histidine residue (His48) within the P1 domain on the other monomer (23). ATP hydrolysis occurs when the P1 domain of one monomer interacts with the ATP-bound P4 domain of the other monomer (24). The interaction of the P1, P3 and P4 domains allow for phosphotransfer to occur and the P5 domain modulates this phosphorylation activity (22). When CheA dimers are in the presence of ATP and Mg^{2+} and in the absence of MCPs, they have a basal level of phosphorylation activity. MCPs and CheW bind to the P5 domain of CheA and modulate its phosphorylation activity relative to basal levels (25, 26). When an MCP is not bound to attractant ligand, this increases CheA phosphorylation by several hundred-fold over the basal level (24). When MCPs are bound by attractant ligand, CheA phosphorylation is decreased

below basal levels (24). Interestingly, this observation is not always seen in other bacteria – in *Bacillus subtilis*, attractant ligand binding to MCPs increases CheA activation (27). The P2 domain of CheA binds to the response regulators CheB and CheY and serves to increase their local concentrations around the P1 domain so that CheA has faster phosphotransfer rates and fast chemotactic responses can be elicited (22). Phosphotransfer from CheA to CheY is faster than to CheB – this ensures that a cellular response is made before adaptation takes place (28). Phosphorylated CheB and CheY have rapid turnover rates and this allows the chemotaxis system to respond quickly to environmental stimuli by regulating the phosphorylation of CheA and phosphate transmission from CheA (22).

CheY is a response regulator that, upon activation by phosphorylation, diffuses to the flagellar motor to cause a change in flagellar rotation, which results in a random change in swimming direction (29). CheY becomes activated when one of its aspartate residues (Asp57) is phosphorylated by CheA (30). Phosphorylation of this residue allows CheY to be captured by the inner C-ring protein of the flagellum called FliM (29, 31). FliM is a component of the switch complex, which also includes the rotor proteins FliG and FliN (29). Phosphorylated CheY then causes a switch in flagellar rotation by interacting with the rotor and the switch complex (29, 32). In *E. coli*, when this happens, the flagella rotate clockwise and the cell tumbles, or changes direction. When CheY is not phosphorylated, the flagella rotate counterclockwise and the cell swims straight (33). Phosphorylated CheY normally has a half-life of about 20 seconds, but this signal is terminated by the phosphatase CheZ, which reduces CheY~P half-life to about 200 milliseconds – this allows for more efficient temporal sensing (2). CheZ functions as a dimer and directly interacts with the active site region of CheY (34). Interestingly, not all chemotactic bacteria have CheZ, as this protein is likely restricted to γ -proteobacteria (2). In these cases,

other mechanisms may exist to allow for proper signal termination, such as additional CheY-like proteins that act as phosphate sinks (35).

CheB is the second response regulator which functions as a methyl-ersterase and removes methyl groups from the MCP to promote adaptation. It consists of an N-terminal CheY-like regulatory domain and a C-terminal catalytic domain (36). CheB is activated when one of its aspartate residues (Asp57) is phosphorylated by CheA, allowing removal of methyl groups from the glutamate residues in the form of methanol (37, 38).

CheR is a constitutively active methyltransferase which methylates glutamate residues within the adaptation region of an MCP. These methyl groups come from *S*-adenosylmethionine. CheR has two binding domains – one for the conserved NWET/SF sequence on the C-terminal end of the MCP and the other at the adaptation region of the MCP (39). When bound to the NWET/SF sequence of the MCP, the ~30 residue flexible arm allows CheR to reach the adaptation sites of 8 nearby MCPs, but not every modifiable glutamate residue (10).

MCP adaptation can be summed up as the methylation state of an MCP in response to environmental stimuli, which determines how sensitive an MCP is to its ligand and if CheA is activated or not. This endows the cell with a molecular memory which goes back in time about 4 seconds (40). When an MCP senses an increasing concentration gradient of attractant, there is no signal transduction to activate CheA which ensures the cell keeps swimming up the gradient and the methylation state of an MCP will keep increasing due to the constitutive activity of CheR. MCPs that are highly methylated have an increased ability to activate CheA and once methylation occurs, the MCP is adapted to the ligand concentration at that point in time. The absence of attractant or presence of repellent will cause the MCP to transmit a signal to activate CheA phosphorylation. The response regulators CheY and CheB will be activated and will cause

the cell to change direction by tumbling, and demethylate the MCPs. MCPs that are demethylated, or deamidated, are less able to activate CheA and once demethylation occurs, the MCP becomes adapted to the new ligand concentration and CheA activity will return to basal levels (2). In *E. coli*, this basal level of signal transduction is the result of mixed populations of MCPs that are in conformations of ligand-on or ligand-off, which is due to the methylation state and its effect on MCP conformation (10).

1.2 Chemotaxis protein cluster formation, stoichiometry and localization patterns

As mentioned earlier, MCPs can form mixed trimers of homodimers, which suggests this is a highly-favored building block for the formation of higher order clusters of large signaling complexes. To achieve a higher level of clustering CheA and CheW proteins are required and together with the MCPs, form stable hexagonal arrays. CheA and CheW form the superlattice which joins the MCPs trimers of dimers together (11). Since this is a very ordered arrangement, stoichiometry of these proteins may be crucial for clustering (41, 42). For example, in *E. coli*, it is predicted that there are 3.4 ± 0.8 MCP dimers to 1.6 CheW proteins to 1 CheA dimer (2, 43). This ratio is not universal, however, and in *Rhodobacter sphaeroides* it is 23.0 ± 4.5 MCP dimers to 1.6 CheW proteins to 1 CheA dimer (43). This discrepancy in the ratios of MCPs to CheA to CheW between these organisms may be connected to the structure of the MCPs and how they are packed into the clusters.

The subcellular localization patterns of the proteins that make up chemotaxis systems can vary depending on the bacterium. *R. sphaeroides* is a rod-shaped bacterium that can be either polarly- or randomly-flagellated and it uses polar or cytoplasmic chemotaxis protein clusters to control its flagellar-based motility (35, 44). Both chemotaxis protein clusters are primarily used

to control the randomly-localized flagellum (35). Having chemotaxis protein clusters localized to distinct sites within the cell may allow for reduced crosstalk between the homologous systems. *R. sphaeroides* has three chemotaxis systems encoded in three operons, cheOp1, cheOp2 and cheOp3, with the latter two being expressed under laboratory conditions. Chemotaxis proteins from cheOp2 and TM receptors localize to polar clusters whereas chemotaxis proteins from cheOp3 and cytoplasmic receptors localize to cytoplasmic clusters (45). The chemotaxis proteins that make up the polar cluster have also been shown to diffuse laterally along the membrane, although the predominant localization is to the poles (46). In young cells, there is one polar cluster and one cytoplasmic cluster at mid-cell. As the cell grows, and right before cell division, an additional polar cluster forms at the other pole so both poles have clusters and another cytoplasmic cluster forms with the old and new clusters localizing to the $\frac{1}{4}$ and $\frac{3}{4}$ positions of the cell (47). This ensures that when the cell divides, each daughter cell will inherit both polar and cytoplasmic clusters. This process of chemotaxis protein cluster formation is believed to be an ordered process. The cytoplasmic cluster formation is known to be dependent on PpfA and TlpT, which are Par-like proteins (7).

Vibrio cholerae is a polarly-flagellated rod-shaped bacterium which forms both cytoplasmic and polar chemotaxis protein clusters (48, 49). The chemotaxis system of *V. cholerae* is encoded in three clusters: I, II and III, with only cluster II shown to be required for chemotaxis (49, 50). When *V. cholerae* is grown in LB broth, in the exponential growth phase cluster II chemotaxis proteins are expressed and localize to the flagellated pole in young cells and a second foci at the other pole develops in older cells before cell division. Cluster I chemotaxis proteins are expressed under low oxygen conditions and localize to the cytoplasm. Cluster III chemotaxis proteins are expressed in stationary phase and under conditions of carbon

starvation. As in *R. sphaeroides*, the process of chemotaxis protein cluster formation and localization is believed to be an ordered process. The proper cluster formation and localization of the polar chemotaxis proteins have been shown to be dependent on ParC and ParP, which are Par-like proteins (48, 51). This group of proteins are described below (section 1.2.2).

E. coli is a peritrichously-flagellated rod-shaped bacterium that forms large chemotaxis protein clusters at the poles and small lateral clusters all along the cell length (47, 52, 53). This bacterium has a single chemotaxis gene cluster for controlling chemotaxis. MCPs are inserted into the inner membrane individually and can nucleate a new cluster or join an existing cluster. As mentioned earlier, MCPs can spontaneously form heterotrimers of homodimers on their own but also interact with CheA and CheW to form higher level clusters. It has been proposed that chemotaxis protein cluster formation is a stochastic process in *E. coli*, and one reason for this is because it does not have cognate Par-like proteins for its chemotaxis protein localization (51). The mechanism by which the polar clusters are held in position is not known but could be due to membrane curvature or phospholipid composition in the inner membrane (47).

These distinct localization patterns are formed using specific localization mechanisms or principles. The localization patterns of chemotaxis proteins are important for proper chemotaxis. For example, in *P. aeruginosa*, the flagellar motor and its corresponding chemotaxis protein cluster are localized to the same pole. If the chemotaxis proteins are mislocalized from the pole of the cell, then the response regulator CheY would have to diffuse a longer distance between CheA and the flagellar motor – this could result in response delays from environmental stimuli. Additionally, localization of chemotaxis proteins may play a role in ensuring that each daughter cell inherits its own protein cluster (47). The Par-like systems that interact with the chemotaxis

proteins mentioned in *V. cholerae* and *R. sphaeroides* are homologous to partitioning systems, which are used for partitioning plasmids and chromosomes upon cell division.

1.2.1 Partitioning systems

One means of localizing bacterial components within the cell is through partitioning (Par) systems. These systems ensure that when a bacterial cell divides, both daughter cells inherit their own copy of the chromosome or plasmid (54, 55). These systems are made up of a ParA NTPase protein, a ParB partition site binding protein, and a *parS* partition site on the chromosome or plasmid where ParB binds (54). ParA proteins can be divided into two types. Type I ParA proteins are typically involved in chromosome and plasmid partitioning and are related to MinD, a protein involved in the spatial regulation of cell division (56). Type I ParA proteins can be further divided into two subgroups: type Ia which have an extended N-terminus that has regulatory activity and type Ib that lack the extended N-terminus (56). Both type Ia and type Ib ParA proteins have Walker Box ATPase activity. Type II ParA proteins are less common, are involved in plasmid segregation, and are related to ParM, which is actin-like and can polymerize (56). ParA functions by binding to ATP, dimerizing and forming filaments and ParB binds to the *parS* site and activates the ATPase activity of ParA (57). Two models have been proposed to describe how plasmids are partitioned. In type I *par* systems, ParB will form a complex with both plasmids in close proximity at mid-cell. ParA then forms filaments where one end is bound to ParB and the other end extends outwards to the ends of the cell while the plasmids are still located mid-cell. The *parS*-bound ParB activates ParA ATPase activity and the filaments disassemble at the ParB end, which results in the plasmids being partitioned, or pulled, to quarter-cell positions (57). In type II *par* systems, after ParB forms a complex with the plasmids,

ParA forms filaments between ParB proteins that are bound to the plasmids. As the ParA filaments extend on both ends, the plasmids are pushed farther apart until they are on opposite sides of the cell. ParB interacts with ParA and activates its ATPase activity and the filaments disassemble, leaving the plasmids at opposite ends of the cell (57). It is typical for *parB* genes to be located directly downstream of their cognate *parA* genes within the same operon in the genome (7). However, there are *parA* homologues are not encoded next to a *parB* gene and these are called orphan *parA* genes. These orphan *parA* genes may not necessarily function in plasmid partitioning, but instead can have other roles. For example, in *Corynebacterium glutamicum*, an orphan ParA protein called PlpP was found to be important for chromosome segregation and cell division as mutants lacking this protein exhibit a division defect, thus demonstrating that ParA proteins can have differing functions aside from chromosome segregation (58, 59). Still, there are other ParA-like proteins that partition large structures such as carboxysomes, which are involved in carbon dioxide fixation (60). Par-like systems, which have homologues of ParA and ParB, have also been shown to be involved in the partitioning and localization of chemotaxis protein clusters in *Vibrio* spp. and *R. sphaeroides* (7, 48, 51).

1.2.2 Par-like systems

In *V. cholerae*, a ParA-like protein called ParC (hereafter ParC_{Vc}) was found to be important for flagellar rotation, swimming motility, and chemotaxis protein localization (48). A *parC_{Vc}* deletion mutant showed a bias towards straight swimming and a 10% reduction in swimming motility (48). The chemotaxis proteins CheW1, an adaptor protein, and CheY3, a response regulator, are encoded in the main *V. cholerae* cluster II chemotaxis operon along with ParC_{Vc} (48). In wild type *V. cholerae*, CheW1 and CheY3 have unipolar localization at the

flagellated pole in young cells and bipolar localization in old cells which ensures that each daughter cell inherits a cluster of these proteins. In a *parC_{Vc}* mutant, 25% of cells had mislocalized CheW1 and CheY3 foci compared to less than 2% for wild type. Increased mislocalization of the chemotaxis proteins away from the flagellum resulted in decreased swimming motility, which highlights the importance of proper intracellular localization for the function of these signal transduction systems. ParC_{Vc} has ATPase activity that is important for its ability to localize and partition CheW1 and CheY3 (48). In *Vibrio parahaemolyticus*, a ParB-like protein designated as ParP (hereafter called ParP_{Vp}) was shown to affect flagellar rotation, swimming motility, and chemotaxis protein localization and partitioning (51). Deletion of *parC_{Vp}* and *parP_{Vp}* from *V. parahaemolyticus* were found to result in a ~25-30% decrease in swimming motility and ~50-60% of cells either having aberrant chemotaxis protein localization or partitioning (51). These proteins directly interact with each other and the histidine kinase CheA, at its localization and inheritance domain (LID) (51). The LID is part of the P2 domain of CheA and is where ParC_{Vp} and ParP_{Vp} bind (51). The fact that ParC_{Vp} and ParP_{Vp} interact with each other further supports the notion that these proteins have homologous function to the ParA and ParB proteins of the Par system. Mutations of conserved residues for ATP binding (Lysine15) and ATP hydrolysis (Glycine11) in ParC_{Vp} impair its ability to interact with CheA and ParP_{Vp} and localize itself, CheW and ParP_{Vp} to the poles. ParP_{Vp} has conserved residues, Tyrosine16 and Tryptophan338, which are needed for interaction with ParC_{Vp} and CheA, respectively, and polar localization of itself and CheA.

In *V. cholerae*, a polar transmembrane anchoring protein called HubP (VC0998) directs ParC as well as two other ATPases, ParA1 and FlhG, to the cell poles upon cell division (61). ParA1 targets *oriCI*, the origin of replication of chromosome I, to the cell pole and FlhG

regulates the assembly of the flagellum. HubP directly interacts with ParA1 and FlhG as was shown by bacterial two-hybrid studies (61). HubP, however, does not interact directly with ParC_{Vc} but instead colocalizes with it (61). Distinct cytoplasmic domains of HubP are required for polar localization of the three ATPases whereas a periplasmic region is required for HubP polar localization. Deletion of *hubP* causes mislocalization of chemotaxis proteins and ParC_{Vc}, loss of ParA1 and FlhG foci formation, a slight increase (6%) in hyperflagellated cells and >50% reduced swimming motility (61). The *hubP* mutant also showed a significant bias towards straight swimming, which likely contributes to the swimming motility defect. These data clearly show the importance of HubP on polar localization of chemotaxis proteins in modulating flagellar-based motility in a polarly-flagellated bacterium.

R. sphaeroides has a ParA-like protein called PpfA that is used for partitioning cytoplasmic chemotaxis proteins through non-specific binding to chromosomal DNA (7). Along with PpfA, the cytoplasmic cluster of chemotaxis proteins is comprised of CheA₃ and CheA₄ histidine kinases, one CheW₄ adaptor protein, and TlpT, a cytoplasmic chemoreceptor (47, 62). Normally, young cells have one cytoplasmic cluster that localizes mid-cell. Old cells develop a second cluster and these clusters localize at the $\frac{1}{4}$ and $\frac{3}{4}$ positions relative to total cell length. The development of a second cluster ensures that each daughter cell will inherit a cytoplasmic chemotaxis protein cluster upon cell division due to the activity of PpfA. In a *ppfA* deletion mutant, this cluster of proteins is not partitioned upon cell division, resulting in only one daughter cell receiving cytoplasmic chemotaxis proteins (7). A small, but significant reduction in swarming motility was also observed in the *ppfA* deletion mutant. Presumably this was due to ~30% of cells not inheriting a cytoplasmic cluster (63). Swarming motility is when bacteria become elongated, hyperflagellated, secrete wetting agents such as rhamnolipids and

coordinately move across a surface in packs (64). Specific amino acid residues in PpfA were shown to be important for chemotaxis protein cluster inheritance and function. These include Glycine10 (dimerization), Lysine14 (ATP binding), Aspartate39 (ATP hydrolysis), and Arginine167/Lysine196 (DNA binding) (7). The cognate ParB-like protein for PpfA is TlpT (Transducer-Like Protein), which is required for chemotaxis protein cluster formation (7).

1.3 *Pseudomonas aeruginosa*

P. aeruginosa is a Gram-negative polarly-flagellated bacterium that is ubiquitous in the environment and commonly found in water, soil and on man-made structures (65). When a person has impaired defenses such as from a burn wound or is immunocompromised, this bacterium may act as an opportunistic pathogen and can cause diseases such as pneumonia, urinary tract infections and bacteremia (66). It also significantly contributes to morbidity and mortality in chronic infections in Cystic Fibrosis (CF) patients (66). CF is a genetic disorder that results in the production of thick and sticky mucus in the lungs, which leads to clogged airways, bacterial infections, lung damage and eventually respiratory failure. *P. aeruginosa* may be the most studied bacterium in regards to CF because of its propensity to cause chronic infections (67). Early in the life of a CF patient, their lungs start to become colonized by several bacterial species, including *P. aeruginosa*. By the time the patient reaches the age of 18 years, *P. aeruginosa* becomes the dominant bacterial isolate in mucus samples as it is present in the lungs of 70+% of patients (67). *P. aeruginosa* infections are challenging to treat as this organism has natural intrinsic resistance. Decreased outer membrane permeability prevents drugs from entering the cells, efflux pumps remove drugs from the cell and there is constitutive expression of β -lactamase, which degrade β -lactam drugs such as ampicillin (68). Lung infections with this

bacterium show increased antimicrobial resistance because it grows in biofilms. Within biofilms, drug molecules have poor diffusion rates, which prevents high concentrations of these molecules from reaching the cells. Antibiotics are usually more effective against metabolically active cells, but cells in a biofilm are less metabolically active, which further contributes to increased antimicrobial resistance (69).

1.3.1 Chemotaxis in *Pseudomonas aeruginosa*

P. aeruginosa has four chemosensory systems that it uses to sense and respond to environmental stimuli such as amino acids, malate, chloroform and oxygen, which may be important for this organism to cause infection in a human host (70, 71). Scattered around its genome are 26 MCP-like genes which are predicted to encode the MCPs required to detect these ligands – at least 13 MCPs have been characterized (71, 72). The chemosensory system gene clusters are located in different parts of the chromosome and have been shown to be involved in swimming motility (*che I* and *che V*), twitching motility (*che IV*), and biofilm formation (*che III*) (73-76). The fourth chemosensory system gene cluster (*che II*) has not been characterized and its function remains unknown, but it encodes for chemotaxis protein homologs. It is known that *che II* genes are expressed in the stationary phase of growth and may be involved in flagellar-mediated behavior (77), although this data has yet to be reproduced. Chemosensory proteins for swimming and twitching motility form foci at the poles of the cell, along with the flagellum and type IV pili, while those involved in biofilm formation form punctate foci anywhere within the cell membrane (77-79). The polar chemotaxis protein localization pattern for swimming motility is also found in *V. cholerae*, another polarly-flagellated bacterium described in section 1.2 (48).

The *che I* and *che V* gene clusters of *P. aeruginosa* encode chemotaxis proteins homologous to those in *E. coli*, which were described above. Cluster *che I* encodes for CheY, CheZ, CheA, CheB, MotC, MotD, ParC (hereafter ParC_{Pa}), ParP (hereafter ParP_{Pa}) and CheW. Cluster *che V* encodes CheR and CheV. Among the chemotaxis proteins listed, CheV does not have a homolog in *E. coli*, yet it is also present in *B. subtilis* and *Salmonella enterica* (80). The function of CheV is poorly understood, although it is believed to be an auxiliary component of chemotaxis systems in human pathogens such as *S. enterica*. CheV has a response regulator and an adaptor domain and therefore could hypothetically interact with CheA and it has been shown to interact with MCPs (80, 81). Interestingly, most of the time, genomes without *cheV* tend to have fewer MCPs than those with *cheV* (80). MotC and MotD function as stators, TM proteins that form proton channels that couple proton flow with the generation of torque within the flagellar motor (82). The ParC_{Pa} and ParP_{Pa} homologs in *P. aeruginosa* have 53% and 43% amino acid sequence identity to ParC_{Vc} and ParP_{Vc} from *V. cholerae* and may have importance in swimming motility and chemotaxis protein localization (48, 51). An alignment of ParC_{Pa} with type Ia, Ib, and II ParA partitioning proteins shows that ParC_{Pa} has a deviant Walker A motif and lacks an N-terminal regulatory region, thus making it more related to type Ib ParA proteins as is PpfA from *R. sphaeroides* and ParC_{Vc} from *V. cholerae* (7).

A polar determinant called the polar organelle coordinator, or POC, complex for the flagellum, type IV pili, and chemotaxis proteins was discovered in *P. aeruginosa* (83). The POC complex consists of three proteins: PA0406 (TonB3), PA2983 (PocA) and PA2982 (PocB), which are currently known to sit at the top of the flagellar localization hierarchy above FlhF (83). In *tonB3*, *pocA*, and *pocB* mutants, FlhF, CheA, and the flagellum are mislocalized from the cell pole. In addition, *tonB3*, *pocA*, and *pocB* mutants are deficient in twitching motility as most cells

do not produce type IV pili or have mislocalized pili. These results show that the POC complex controls two separate motility systems. PocA and PocB form a membrane-associated complex and localize to the cell periphery where they dictate the localization of polar proteins, but the localization of TonB3 has yet to be determined. After the POC complex, FlhF is above all other known proteins for flagellar localization, including CheA (84). FlhF is a polar GTPase that is required for the polar localization of the flagellar apparatus (85). Deletion of *flhF* results in cells that have mislocalized chemotaxis proteins and flagella, which results in reduced swimming motility (83). Aside from FlhF and the Poc complex, there are no other major polar determinants of the chemotaxis system proteins known in *P. aeruginosa*. In cells treated with a chemical to inhibit cell division, *P. aeruginosa* cells form long filaments and chemotaxis protein clusters form mid-cell in addition to the poles, thus demonstrating that other undiscovered mechanisms may exist for cluster localization (83). A homologue of the *V. cholerae* polar anchoring protein HubP was found in *P. aeruginosa* that is called FimV (61). FimV is involved in twitching motility (86), however, there is currently no published research showing that FimV is involved in chemotaxis.

1.4 The second messenger c-di-GMP

Bis-(3'→5')-cyclic dimeric guanosine monophosphate, or c-di-GMP is a bacterial second messenger that has been shown to regulate biofilm formation, differentiation, motility and virulence (87). Second messengers are molecules that relay signals sensed by a receptor to an effector protein which in turn mediates a cellular response. C-di-GMP molecules are synthesized from 2 GTP molecules by enzymes called diguanylate cyclases, or DGCs (88). Many of these DGC enzymes have an autoinhibitory site, or I-site, that binds c-di-GMP to prevent excess

production of this molecule (89). This negative feedback allows the cell to regulate how much c-di-GMP is available to activate effector (c-di-GMP binding) proteins. In *P. fluorescens*, mutation of certain residues within the I-site of GcbA, a DGC, reduces the strength of the interaction with LapD, an effector protein required for biofilm formation (89). These results suggest that DGC binding to effector proteins may aid in preventing crosstalk to other effector proteins that bind c-di-GMP. DGCs can be identified by the presence of a conserved GGDEF domain. Conversely, there are other enzymes that can degrade c-di-GMP and these are known as phosphodiesterases, or PDEs (88). There are two main types of PDEs and they function by degrading c-di-GMP in different ways. One type converts c-di-GMP into linear di-GMP, or 5'-pGpG, and this type contains a conserved EAL domain (87). The second type converts c-di-GMP into 2 GMP molecules and contains a conserved HD-GYP domain (87). *P. aeruginosa* has 43 genes which encode for proteins with GGDEF, EAL or HD-GYP domains and of these, 33 have a GGDEF domain, 24 have an EAL domain and 3 have an HD-GYP domain (90-93). While many of these proteins have been confirmed to have DGC or PDE activity, there are still others that remain uncharacterized (92, 94, 95). There are proteins that have both a GGDEF and an EAL domain, but usually only one of the domains is catalytically active while the other domain gains a regulatory function (93). Interestingly, in *Agrobacterium tumefaciens*, a protein called DcpA was discovered that has both GGDEF and EAL domains and both DGC and PDE activity (96). In *P. aeruginosa* PAO1, the dual GGDEF and EAL domain-containing protein MucR functions as a DGC in planktonic cells for alginate production and a PDE in biofilm cells for biofilm dispersion (93, 97, 98).

1.4.1 C-di-GMP and its impact on chemotaxis

In regards to chemotaxis and biofilm formation, c-di-GMP levels are widely known to dictate the switch between motile (planktonic) and sessile (biofilm) states of growth. The mechanisms by which c-di-GMP levels influence this decision are not well characterized in most bacteria. In *E. coli* and *Salmonella Typhimurium*, a c-di-GMP effector protein called YcgR is able to bind c-di-GMP and interact with the flagellar motor to reduce flagellar reversals and reduce cell velocity (29, 99-101). In *P. aeruginosa* PA14, c-di-GMP levels have been shown to influence which stator pairs interact with the flagellar motor and this can affect swarming motility (102). As mentioned earlier, stators are TM proteins which are part of the flagellar motor and are involved in the generation of torque for the flagellum. The stator pairs of *P. aeruginosa* are MotA/B and MotC/D. Both stator sets can be used for swimming motility yet MotC/D are used primarily for swarming motility. When c-di-GMP levels are high in the cell, the MotA/B stator can displace MotC/D and this can affect motor function in regards to swarming motility (103). It has been proposed that interactions between MotA and FliG are required for swarming repression by MotA, but a direct protein-protein interaction between these proteins was not seen (103).

When a *P. aeruginosa* cell divides, only one daughter cell will inherit the flagellum, whereas the other daughter cell will synthesize a new one (104). Recent studies in *P. aeruginosa* PA14 have shown that individual cells exhibit c-di-GMP heterogeneity due to the asymmetrical inheritance of a phosphodiesterase called DipA or Pch (hereafter DipA) (84). The daughter cell that inherits the flagellum also inherits the DipA cluster, which lowers the c-di-GMP levels in that cell as compared to the other daughter cell without a DipA cluster. The polar localization of DipA was found to be completely dependent on the chemotaxis histidine kinase CheA and the

phosphorylation of CheA promoted DipA PDE activity. The polar localization of the flagellum requires the GTPase, FlhF. FlhF is also required for polar localization of CheA and DipA, but not their association with each other (84). This suggests that the flagellum, CheA and DipA form a complex at one pole of the cell. Using a pulldown method, CheA was found to co-precipitate with DipA, thus demonstrating that these proteins form a complex (84). However, the pulldown method cannot determine if the CheA-DipA interaction is direct or through an intermediate. In *P. aeruginosa* PA68, the absence of DipA results in a defect in swimming motility and swarming motility (105). This defect was observed in a bulk population assay, yet the actual mechanism for how these swimming and swarming motility defects occurred was unknown. More recent studies of a *dipA* mutant revealed that most cells had high levels of c-di-GMP, and a reduction in average cell velocity and flagellar reversals compared with wild type. These results suggest that c-di-GMP modulates cell velocity and flagellar reversals, but the mechanism by which this occurs is unknown (84). As mentioned earlier, *E. coli* and *S. Typhimurium* have an effector protein called YcgR that binds c-di-GMP and the flagellar motor to cause a reduction in cell velocity and flagellar reversals. In *P. aeruginosa*, an effector protein may cause the reduction in motility in a *dipA* mutant, but this protein has yet to be identified.

1.5 Biofilm dispersion

Biofilms are a form of growth wherein the cells are non-motile, or sessile, and exist in an extracellular matrix of DNA, proteins, and polysaccharides (106). Bacterial cells in a biofilm are non-motile and flagellar gene transcription is inhibited (107). This form of growth allows cells to slow their metabolic rate and persist in this matrix for long periods of time. Additionally, it is much more difficult for antimicrobial agents to diffuse into biofilms to kill bacteria. While there are obvious benefits to growing in a biofilm, bacteria cells can revert back to planktonic growth. Environmental signals such as glutamate, glucose or succinate trigger *P. aeruginosa* to switch from a biofilm to a planktonic mode of growth – this process is known as biofilm dispersion. During biofilm dispersion, the extracellular matrix of the biofilm is broken down, flagellar gene expression and motility is increased, and cell adhesion is reduced (108-111). To date, several proteins have been implicated in biofilm dispersion and two pathways have been proposed in *P. aeruginosa*. The dual DGC and PDE protein MucR of *P. aeruginosa* is required for nitric oxide and glutamate-induced biofilm dispersion (97, 98). In biofilm cells, MucR acts as a PDE, lowering c-di-GMP levels and causing biofilm dispersal. The mechanism by which MucR is activated to perform this function remains to be elucidated. In *P. aeruginosa* PAO1, the membrane-bound DGC NicD is normally phosphorylated and inactive (95). When NicD senses an environmental cue such as glutamate, it becomes dephosphorylated and its DGC activity increases, resulting in higher cellular levels of c-di-GMP (95). Along with the elevated c-di-GMP levels, the chemotaxis transducer-like protein BdlA becomes phosphorylated and is subsequently proteolytically cleaved in a non-processive manner requiring the protease ClpP and chaperone ClpD (112). This modified form of BdlA is now active and enhances the PDE activity of DipA, which subsequently lowers c-di-GMP levels in the cell, resulting in biofilm dispersion

(111). A second PDE, RbdA, has been shown to interact with BdlA *in vivo* and is proposed to contribute to the decrease in c-di-GMP in response to BdlA activation (111). The localization of DipA has not yet been determined in biofilm or biofilm-dispersed cells.

1.6 Concluding remarks

The loss of chemotaxis protein cluster formation or inheritance reduces chemotaxis and can have a positive or negative impact on the virulence of a bacterium. Bacteria have evolved various mechanisms to ensure that chemotaxis protein clusters are formed and localized at specific regions within the cell. These mechanisms may be stochastic in nature, as what appears to be the case for *E. coli*, or they can be ordered. Chemotaxis proteins, like chromosomes and plasmids, may need systems in place to ensure that they are localized properly for optimal chemotaxis and that daughter cells inherit their own clusters for use after cell division. Par-like proteins have been implicated in the partitioning and localization of chemotaxis proteins and the chemotactic ability of *Vibrio spp.* and *R. sphaeroides* (7, 48, 51). Since *P. aeruginosa* is an opportunistic pathogen and chemotaxis is needed for its ability to cause disease, we examined the role of the Par-like proteins in this bacterium. In our studies, we determined what effect the loss of the Par-like proteins had on swimming motility and chemotaxis protein cluster formation and localization. The ATPase domain of ParC was investigated to see if it was important for swimming motility. We performed a bacterial two-hybrid assay to identify proteins that interact with the Par-like proteins. Finally, we examined the interdependence on cluster formation of the Par-like proteins with a chemotaxis protein and a c-di-GMP phosphodiesterase that is involved in chemotaxis and biofilm dispersion. Our experiments show that the Par-like protein ParP may be involved in biofilm dispersion and further studies must be performed to confirm this.

Chapter Two

Materials and Methods

2.1 Strains, plasmids, growth conditions and media used

Lists of plasmids and strains made and used in this publication are in Tables 2.1 and 2.2, respectively. All *P. aeruginosa* strains generated in the work are derived from *P. aeruginosa* PAO1 (Iglewski strain – obtained from Carrie Harwood, University of Washington). Both *E. coli* and *P. aeruginosa* were grown in Lysogeny Broth (LB) with aeration and on LB 1.5% agar plates at 37°C. Antibiotics were used at the following concentrations as appropriate: 30 or 50 µg/mL of gentamycin and 70 µg/mL of tetracycline for *P. aeruginosa* and 15 µg/mL of gentamycin, 30 µg/mL of kanamycin, 25 µg/mL of chloramphenicol and 10 µg/mL of tetracycline for *E. coli*.

Table 2.1 Plasmids used in this study

Plasmid	Description	Source
$\Delta cheA$:pEX18Tc	DNA fusion product for deletion of <i>cheA</i> cloned into the EcoRI (5') and BamHI (3') sites of pEX18Tc	This study
$\Delta cheW$:pEX18Tc	DNA fusion product for deletion of <i>cheW</i> cloned into the EcoRI (5') and BamHI (3') sites of pEX18Tc	This study
$\Delta dipA$:pEX18Tc	DNA fusion product for deletion of <i>dipA</i> cloned into the EcoRI (5') and SacI (3') sites of pEX18Tc	This study
$\Delta parC$:pEX18Tc	DNA fusion product for deletion of <i>parC</i> cloned into the EcoRI (5') and BamHI (3') sites of pEX18Tc	This study
$\Delta parP$:pEX18Gm	DNA fusion product for deletion of <i>parP</i> cloned into the EcoRI (5') and HindIII (3') sites of pEX18Gm	This study
<i>cheA-mTq</i> :pEX18Gm	DNA fusion product for insertion of <i>cheA-mTurquoise</i> at the native chromosomal site, cloned into pEX18Gm	(84)
<i>dipA-yfp</i> :pUC18T-mini-TN7T-Gm	Plasmid template for amplifying <i>dipA-yfp</i>	(84)
pJN105	Broad host range vector. pBBR-1 MCS5 AraC-pBAD derivative	(113)
his- <i>cheW</i> :pJN105	his- <i>cheW</i> cloned into the EcoRI (5') and SacI (3') sites of pJN105	This study
his- <i>dipA</i> :pJN105	his- <i>dipA</i> cloned into the EcoRI (5') and XmaI (3') sites of pJN105	This study
<i>parC</i> :pJN105	<i>parC</i> cloned into the EcoRI (5') and XbaI (3') sites of pJN105	This study
<i>parC</i> -his:pJN105	<i>parC</i> -his cloned into the EcoRI (5') and XbaI (3') sites of pJN105	This study
his- <i>parP</i> :pJN105	his- <i>parP</i> cloned into the EcoRI (5') and SacI (3') sites of pJN105	This study
his- <i>parP-cheW</i> :pJN105	his- <i>parP-cheW</i> cloned into the EcoRI (5') and SacI (3') sites of pJN105	This study
his- <i>cheW</i> -PA1465:pJN105	his- <i>cheW</i> -PA1465 cloned into the EcoRI (5') and SacI (3') sites of pJN105	This study

Table 2.1 (Cont.) Plasmids used in this study

Plasmid	Description	Source
<i>dipA-yfp</i> :pJN105	<i>dipA-yfp</i> amplified from <i>dipA-yfp</i> :pUC18T-mini-TN7T-Gm and cloned into the EcoRI (5') and XbaI (3') sites of pJN105	This study
<i>yfp-parP</i> :pJN105	DNA fusion product <i>yfp-parP</i> cloned into the EcoRI (5') and SacI (3') sites of pJN105	This study
pBT	Expression vector used for Bacterial Two-Hybrid	Agilent Technologies
pTRG	Expression vector used for Bacterial Two-Hybrid	Agilent Technologies
<i>cheA</i> :pTRG	<i>cheA</i> cloned into the BamHI (5') and EcoRI (3') sites of pTRG	This study
<i>dipA</i> :pBT	<i>dipA</i> cloned into the NotI (5') and EcoRI (3') sites of pBT	This study
<i>mcpS</i> :pTRG	<i>mcpS</i> cloned into the XhoI (5') and NotI (3') sites of pTRG	This study
<i>parC</i> :pBT	<i>parC</i> cloned into the NotI (5') and EcoRI (3') sites of pBT	This study
<i>parC</i> :pTRG	<i>parC</i> cloned into the NotI (5') and EcoRI (3') sites of pTRG	This study
<i>parP</i> :pBT	<i>parP</i> cloned into the NotI (5') and EcoRI (3') sites of pBT	This study
tPA2867:pTRG	tPA2867 cloned into the EcoRI (5') and XhoI (3') sites of pTRG	This study
tPA4290:pTRG	tPA4290 cloned into the EcoRI (5') and XhoI (3') sites of pTRG	This study

Table 2.2 Strains used in this study

Strain	Description	Source
<i>E. coli</i> BacterioMatch II Two-Hybrid System Reporter Strain	$\Delta(mcrA)183 \Delta(mcrCB-hsdSMR-mrr)173 endA1 hisB supE44 thi-1 recA1 gyrA96 relA1 lac [F' lacI^q HIS3 aadA Kan^r]$	Agilent Technologies
<i>E. coli</i> XL-1 Blue MRF' kan ^r	$\Delta(mcrA)183 \Delta(mcrCB-hsdSMR-mrr)173 endA1 supE44 thi-1 recA1 gyrA96 relA1 lac [F' proAB lacI^q Z\Delta M15 Tn5 (Kan^r)]$	Agilent Technologies
<i>E. coli</i> XL-1 Blue MRF' tet ^r	$recA1 endA1 gyrA96 thi-1 hsdR17 supE44 relA1 lac [F' proAB lacI^q Z\Delta M15 Tn10 (Tet^r)]$	Agilent Technologies
<i>E. coli</i> S17-1	$Tp^R Sm^R recA thi pro hsdR M+ RP4 2-Tc::Mu-Km::Tn7 \lambda pir$	(114)
<i>E. coli</i> NEB5 α	$fhuA2 \Delta(argF-lacZ)U169 phoA glnV44 \Phi80 \Delta(lacZ)M15 gyrA96 recA1 relA1 endA1 thi-1 hsdR17$	New England Biolabs
PAO1	<i>P. aeruginosa</i> PAO1 (Iglewski strain)	Carrie Harwood
PAO1 <i>cheA-mTq</i>	<i>cheA-mTq</i> at the native chromosomal site in PAO1	This study
PAO1 $\Delta cheA$	In-frame deletion of PA1458 (<i>cheA</i>) in PAO1	This study
PAO1 $\Delta cheW$	(+9) deletion of PA1464 (<i>cheW</i>) in PAO1	This study
PAO1 $\Delta che I$	In-frame deletions of PA1456 (<i>cheY</i>), PA1457 (<i>cheZ</i>), PA1458 (<i>cheA</i>), PA1459 (<i>cheB</i>), and PA1464 (<i>cheW</i>) in PAO1	Carrie Harwood
PAO1 $\Delta dipA$	(+9) deletion of PA5017 (<i>dipA</i>) in PAO1	This study
PAO1 <i>fliC::tn</i>	Transposon (lacZ _{hah}) in PA1092 (<i>fliC</i>) in PAO1. Inserted at base 820 of 1467	University of Washington PAO1 transposon mutant collection
PAO1 $\Delta parC$	In-Frame deletion of PA1462 (<i>parC</i>) in PAO1	This study
PAO1 $\Delta parP$	(+9) deletion of PA1463 (<i>parP</i>) in PAO1	This study

2.2 Generation of deletion mutants and expression strains

In-frame gene deletions of *cheA* and *parC* were generated by homologous recombination using the suicide vectors pEX18Tc or pEX19Gm (115). Briefly, 1 Kb DNA fragments upstream and downstream of the genes of interest were PCR amplified and fused together by splice overlap extension PCR using PAO1 DNA as template (116). Primers are listed in Table 2.3. These constructs were sequenced to ensure no undesired mutations were introduced. This resultant fragment was cloned into pEX18Tc or pEX19Gm and transformed into *E. coli* S17-1 for mating into *P. aeruginosa* PAO1. Merodiploids were selected on tetracycline or gentamycin, as appropriate, with chloramphenicol [5 µg/mL] providing counter-selection against *E. coli*. Resolution of the merodiploids was achieved through 10% sucrose counter-selection. The deletions were then confirmed by PCR. Gene deletions of *cheW*, *dipA*, and *parP* were performed as above except both the upstream and downstream 1 Kb DNA fragments also had nine base pairs from the 5' and 3' ends of the gene, respectively. This deletion (+9) resulted in the first and last nine bases pairs of each gene being fused together so that a five-amino acid peptide would be expressed and thus reduce the likelihood of polar effects.

The strains with *cheA-mTq* incorporated at the native site of the chromosome were made using a *cheA-mTq*:pEX19Gm construct (84) as above. In this construct, *cheA* from *P. aeruginosa* PA14 was used. The CheA amino acid sequences from strains PAO1 and PA14 are 99.6% identical, with three residues [E133A, A161V and P191S, respectively] being different between them. The *dipA* gene from *dipA-yfp*:pJN105 is from PA14, but the amino acid sequence matches PAO1.

2.3 Site-directed mutagenesis

A single point mutation of K15A in *parC* was generated by site-directed mutagenesis. PCR was performed using *parC*:pSB109 as template and the appropriate mutagenic primers (Table 2.3). This PCR product was digested with DpnI (New England Biolabs) for 1 hour at 37°C and transformed into *E. coli* NEB5 α cells. The *parC-K15A* gene insert was sequenced to confirm that the mutation was present and this insert was sub-cloned into pJN105 and transformed into PAO1 and Δ *parC_{Pa}* for complementation studies.

Table 2.3 Primers used in this study

Primer name	Sequence (5' to 3')
Gene deletion	
<i>cheA</i> (Up)-for	GCGACGAATTCGAATCGACCCTG
<i>cheA</i> (Up)-rev	CGGAAACCCATACGCGGCGTCGGCTGCTCCCAGAGACGTG
<i>cheA</i> (Dn)-for	CACGTCTCTGGGAGCAGCCGACGCCGCGTATGGGTTTCCG
<i>cheA</i> (Dn)-rev	GAGGATCCCTGCTTGAGCAGGCGCGCAC
<i>cheW</i> (Up)-for	GCGACGAATTCAGGCGCATTCAAGCCGCAC
<i>cheW</i> (Up)-rev	GTAGAACGCATCAGATGCTTTTGCTCATTCCCCTAACC
<i>cheW</i> (Dn)-for	GGTTAGGGGAATGAGCAAAGCATCTGATGCGTTCTAC
<i>cheW</i> (Dn)-rev	GAGGATCCCTGGCCATTCTCCAGCACC
<i>dipA</i> (Up)-for	ATAGGAATTCATCACCGACATGGAAGCCTTC
<i>dipA</i> (Up)-rev	GCCTGGGCGATCAGTGCAGACTTTTCATGCGAGGCTGATT CC
<i>dipA</i> (Dn)-for	GAATCAGCCTCGCATGAAAAGTCTGCACTGATCGCCCAGG C
<i>dipA</i> (Dn)-rev	GAAAGAGCTCGCGCCAGCTCAAGCGTTTC
<i>parC</i> (Up)-for	GAGAATTCACGAACGCTGGCTGGTTTC
<i>parC</i> (Up)-rev	CGGCGACCGGCGCGCCATGCTCTACTCTTCCCTGGCATG
<i>parC</i> (Dn)-for	CATGCCAGGAAGAGTAGAGCATGGCGCGCCGGTCGCCG
<i>parC</i> (Dn)-rev	GAGGATCCCTATCAATGGTCGCCGTGCAG
<i>parP</i> (Up)-for	GAGATGAATTCGTCGCCTTCGCCATGAGCG
<i>parP</i> (Up)-rev	GAAGCTGTCTATCAATGGTCGGCGCTCATGTGGGTATTCC
<i>parP</i> (Dn)-for	GGAATACCCACATGAGCGCCGACCATTGATAGACAGCTTC CG
<i>parP</i> (Dn)-rev	GAGATAAGCTTGAAGTGGCGAGCCGCCTG
Bacterial two-hybrid	
<i>cheA</i> -pTRG-for	GCGGATCCATGAGCTTCGACGCCGATGA
<i>cheA</i> -pTRG-rev	CGGAATTCAGTCTACGCGGCACGCATTG
<i>dipA</i> -pBT/TRG-for	AGACGCGGCCGCTATGAAAAGTCATCCCGATGCCGCC
<i>dipA</i> -pBT/TRG-rev	ATTGGAATTCTCAGTGCAGGGTGCGGCAG
<i>mcpS</i> -pBT/TRG-for	GGGATCCCGATGCTCTTCGGCAGAAAAG
<i>mcpS</i> -pBT/TRG-rev	GGCTCGAGCTTGAACAGGCTCGACACCAC
<i>parC</i> -pBT/TRG-for	AGCGGCCGCTATGAAAGTCTGGGCAGTCG
<i>parC</i> -pBT/TRG-rev	ATACGAATTCTCAGGCCACCCGGGTGGC
<i>parP</i> -pBT/TRG-for	AGCGGCCGCTATGAGCGCCGCCACCGCC
<i>parP</i> -pBT/TRG-rev	ATACGAATTCTCAATGGTCGCCGTGCAGG
tPA2867-pTRG-for	ATACGAATTCTTTTCATCCTCACCCACCTGC
PA2867-pBT/TRG-rev	ATACCTCGAGTCAGAGGCGTAGCTGGCCG
tPA4290-pTRG-for	ATACGAATTCTTCTGTACCTGGCCCTGCCGC
PA4290-pBT/TRG-rev	ATACCTCGAGCTAGCCGTTCAAGGCCAGGC
Site-directed mutagenesis^a	
<i>parC</i> -K15A-for	GAAAGGAGGGGT CGGCGCG ACCACCTCGTCCATCG
<i>parC</i> -K15A-rev	CGATGGACGAGGTGGT CGCGCCG ACCCCTCCTTTC

^aMutagenic codons are in bold.

Table 2.3 (Cont.) Primers used in this study

Primer name	Sequence (5' to 3')
Complementation	
<i>his-cheW</i> -for	GTTAAGAATTCATGCACCACCATCACCACCATAGCAAAGCCA CCGCGCAAAGC
<i>cheW</i> -rev	CTAGAGCTCTCAGATGCTGCCAGCTCCG
<i>his-dipA</i> -for	TTCAGAATTCATGCACCACCATCACCACCATAAAAGTCATCC CGATGCCGCC
<i>dipA</i> -rev	TGCCCGGGTCAGTGCAGGGTGCGGCAG
<i>parC</i> -for	GTTAAGAATTCATGAAAGTCTGGGCAGTCGC
<i>parC</i> -rev	CTATCTAGAACTCCGGTGCGGCTTGAATG
<i>parC</i> -his-rev	CTATCTAGATCAATGGTGGTGGTGGTGGGCCACCCGGGT GGCCGGC
<i>his-parP</i> -for	GTTAAGAATTCATGCACCACCATCACCACCATAGCGCCGCCA CCGCCACCC
<i>parP</i> -rev	CTAGAGCTCTCAATGGTCGCCGTGCAGG
PA1465-rev	CTAGAGCTCTCACTTGCCCTTGGCTTCGTG
Fluorescence microscopy	
<i>dipA(yfp)</i> -for	TTCAGAATTCATGAAAAGTCATCCCGATGCCG
<i>yfp(dipA)</i> -rev	CTATCTAGATTACTTGTACAGCTCGTCCATG
<i>yfp(parP)</i> -for	ATTGGAATTCATGGTGAGCAAGGGCGAGGAG
<i>yfp(parP)</i> -rev	GTGGCGGTGGCGGCGCTCATCTTGTACAGCTCGTCCATGCC
<i>parP(yfpA)</i> -Dn-for	CATGGACGAGCTGTACAAGATGAGCGCCGCCACCGCCAC
<i>parP(yfpA)</i> -Dn-rev	GAAGAGCTCTCAATGGTCGCCGTGCAGG

2.4 Growth curves

Overnight cultures of *P. aeruginosa* strains were diluted to $OD_{600nm} = 0.05$ in 50 mL of LB with gentamycin, 50 $\mu\text{g/mL}$, and incubated at 37°C with aeration. OD_{600nm} readings were taken approximately once every hour.

2.4 Bacterial two-hybrid analysis

Strains were constructed and protein interactions were tested using the BacterioMatch II Two-Hybrid System Library Construction Kit instruction manual (Agilent Technologies). Briefly, the overnight cultures were diluted to equal cell density. Five ten-fold serial dilutions of each culture were made and 5 μl of each was spotted on non-selective and dual-selective plates containing antibiotics and IPTG. The dual-selective plates had 5 mM 3-AT and 10 $\mu\text{g/ml}$ streptomycin to test the strength of the protein interactions. The negative control strain harbored empty pBT and pTRG vectors, while the positive control strain harbored *lgf2*:pBT and *gallI*:pTRG as supplied by the manufacturer. The pBT and pTRG constructs were made using standard cloning techniques and transformed into *E. coli* XL1-Blue MRF' Kan^R or Tet^R cells. The genes used in this assay were *parC*, *parP*, *cheA*, *dipA*, *mcpS*, PA2867 and PA4290. PA2867 and PA4290 are both transmembrane receptors, and so truncated versions (tPA2867₁₆₁₋₄₉₀ and tPA4290₃₃₋₅₃₈) containing only the C-terminal cytoplasmic portion were used to ensure these recombinant proteins could reach the reporter cassette on the chromosome. Strains for B2H assays were made by co-transforming the recombinant pBT and pTRG constructs into the *E. coli* BacterioMatch II Two-Hybrid System Reporter Strain.

2.5 SDS-PAGE and western blot

Overnight cultures of *P. aeruginosa* were diluted 1:100 in LB broth and incubated for three hours with antibiotics, as appropriate, and aeration at 37°C, resulting in cultures in mid/late log phase (OD_{600nm} 0.5 - 1). The cells were harvested and suspended in 2X SDS loading buffer, and loading was normalized based on OD_{600nm}. Whole cell lysates were separated by SDS-PAGE on 10, 12 or 15% gels, and stained using Coomassie brilliant blue G-250 - perchloric acid solution (117). The primary antibodies were α -His (1:3000), α -mCherry (1:1000) and α -GFP (1:1000). Secondary antibodies (1:10000) were conjugated to peroxidase to allow detection of signal using the SuperSignal West Femto Maximum Sensitivity Substrate kit. Western blots were visualized and imaged using a Fotodyne FOTO/Analyst FX system.

2.6 Swimming assay

P. aeruginosa strains harboring pJN105 constructs were streaked on LB media with antibiotics for isolation and incubated overnight at 37°C. Fresh colonies were stab inoculated into swimming media (1% tryptone, 0.5% NaCl and 0.3% agar) with antibiotics. These plates were incubated at 30°C for 18 hours, after which measurements of the diameter of the swimming zones were obtained. For each assay, 12 biological replicates were performed. ANOVA calculations were followed by the Tukey HSD post-hoc test using the R Console program (Version 3.2.3).

2.7 Flagellin preparation assay

Flagella were sheared from the bacterial cell surface similarly as described for type IV pili (118). Overnight cultures of *P. aeruginosa* PAO1 grown at 37°C in LB broth with aeration

had their OD_{600nm} measured and cells were harvested at 4000 x g for 10 minutes. The cell pellets were resuspended in 1 ml of 0.15 M NaCl and 0.2 % formaldehyde in Eppendorf tubes. The OD_{600nm} of each sample was normalized to the lowest one obtained and ranged from 10 to 50, depending on how many OD units were harvested. The cultures were vortexed at high speed for 30 minutes to shear flagella from the cells. Intact cells and membranes were removed via centrifugation and the sheared proteins were precipitated overnight in 100 mM MgCl₂ at 4°C. The sheared proteins were collected by centrifugation at 16800 x g for 15 minutes and resuspended in 25 µl 2X SDS loading buffer. These samples were separated by SDS-PAGE on a 10% gel and all proteins were stained by Coomassie G-250-perchloric acid solution (117).

2.8 Fluorescence microscopy

Overnight cultures of *P. aeruginosa* were diluted 1:100 in LB broth and incubated for three hours with antibiotics, as appropriate, and aeration at 37°C, resulting in cultures in mid/late log phase (OD_{600nm} between 0.5 and 1). 5 µl of culture was spotted onto a polylysine-treated coverslip (Fisherbrand 25CIR-1D) for observation using a Nikon Eclipse 90i microscope with a Hamamatsu digital camera C11440 (ORCA-Flash 4.0) and a Nikon Intensilight C-GHFI halogen lamp. Images were captured under DIC, Yfp, and Cfp filters, as appropriate. For quantitation of localization patterns, between 248 and 300 cells were scored for foci formation and localization. Foci were labeled as being polar if they fell within the curvature of the poles or non-polar if they did not.

2.9 Protein alignment

Clustal Omega multiple sequence alignment was used for comparing the amino acid sequences of multiple proteins (119).

Chapter Three

Results

3.1 Par-like proteins are required for optimal chemotaxis in *Pseudomonas aeruginosa*

The chemotaxis gene cluster (*che I*) of *P. aeruginosa* encodes most of the genes required for chemotactic control of flagellar-based motility (74). This includes the *par*-like genes *parC_{Pa}* and *parP_{Pa}* (Figure 3.1A). Homologs of these genes are found in other polarly-flagellated non-Enterobacteriaceae γ -proteobacteria such as *V. parahaemolyticus* (51). It has been shown in *V. parahaemolyticus* that deletion of *parC_{Vp}* and *parP_{Vp}*, individually or combined, resulted in a ~25-30% defect in swimming motility. This swimming defect in each deletion was due to an increase in the percentage of the cell population that lack chemotaxis protein foci or have mislocalized chemotaxis protein foci (51). These results imply that ParC_{Vp} and ParP_{Vp} work in the same pathway. Due to the amino acid sequence homology between ParC and ParP in *V. parahaemolyticus* and *P. aeruginosa* and the conserved genetic organization surrounding these genes, ParC_{Pa} and ParP_{Pa} were proposed to be important for swimming motility in *P. aeruginosa*. Deletion of *parC_{Pa}* and *parP_{Pa}* resulted in a 25% and 70% reduction in swimming motility, respectively, and could be partially complemented with His-tagged fusion proteins (Figure 3.1B). These results suggested that ParP_{Pa} has a more important role in chemotaxis than ParC_{Pa}. The *fliC::tn* mutant acts as a negative control in this assay in that it is non-flagellated. The *che I* mutant is the deletion of the *che I* cluster chemotaxis genes *cheY*, *cheZ*, *cheA*, *cheB*, and *cheW*, and acts as a negative control in that it is non-chemotactic. A growth curve showed that the *par*-like gene mutants have a similar growth rate as wild type, which showed that the swimming defect is not due to a growth defect (Figure 3.2). Given that the swimming defects seen in the *parC_{Pa}* and *parP_{Pa}* mutants could result from either a loss of chemotaxis or a defect in flagellation, the focus shifted to determining the function of ParC_{Pa} and ParP_{Pa} and why the defect in the *parP_{Pa}* mutant was greater.

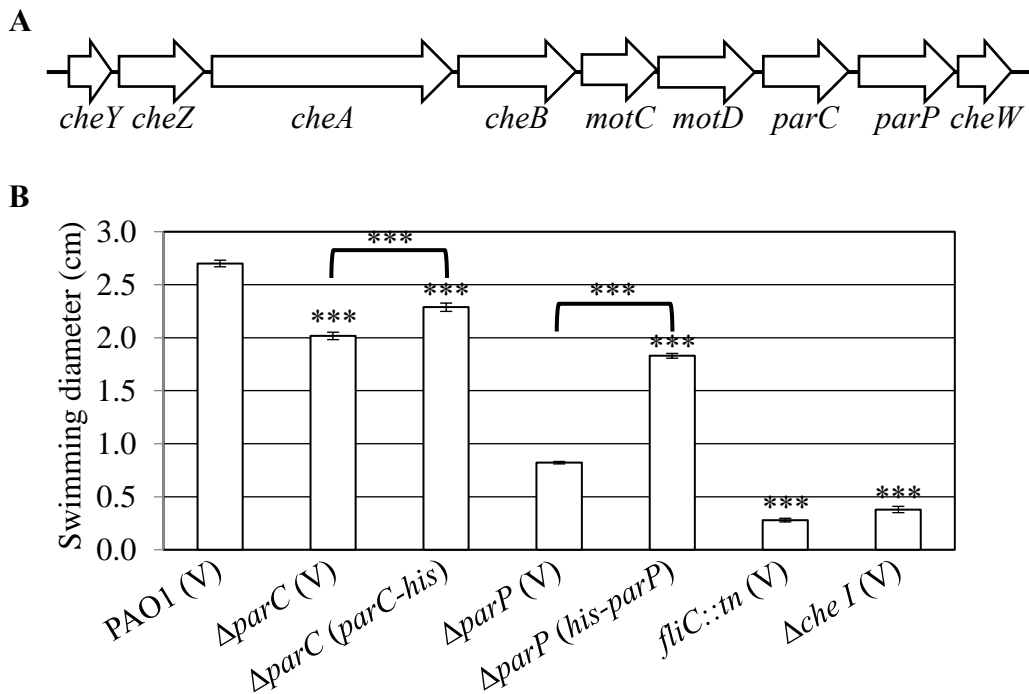


Figure 3.1 – Par-like proteins are encoded within chemotaxis gene cluster I (*che I*) and are required for optimal swimming motility. (A) *che I* of *P. aeruginosa* - drawn to scale. (B) Swimming motility assay of wild type and indicated *P. aeruginosa* strains. The average swimming diameter measurements are shown and error bars denote the standard error of the mean. *** = $p < 0.0001$ compared to wild type.

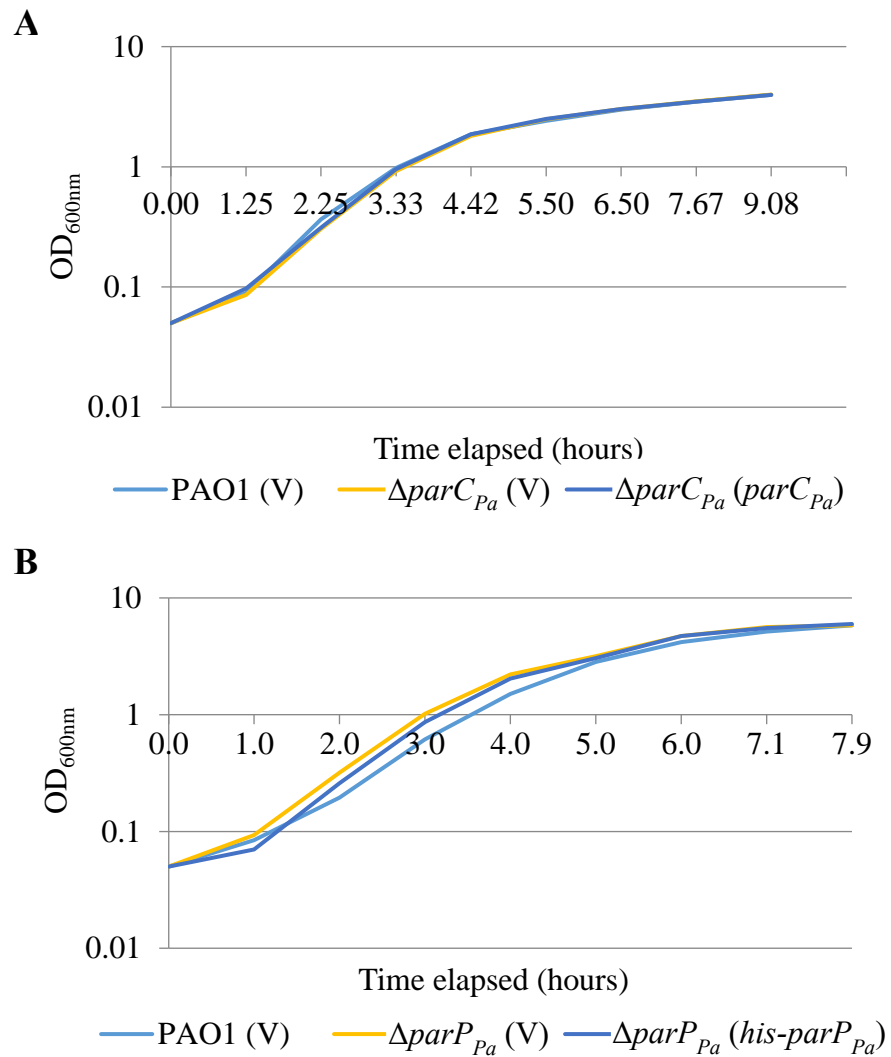


Figure 3.2 – *parC_{Pa}* and *parP_{Pa}* mutants do not have a defect in their growth rate. Growth curve assays of (A) *parC_{Pa}* and (B) *parP_{Pa}* mutants with complementation.

3.2 Chemotaxis protein localization is dependent on the Par-like proteins

To determine the cause of the swimming motility defects in the *parC_{Pa}* and *parP_{Pa}* mutants, we examined chemotaxis protein localization and expression, and surface flagellin levels. The chemotaxis proteins of *P. aeruginosa* normally localize to the poles of the cell (77). It has been previously demonstrated that in *V. parahaemolyticus*, deletion of *parC_{Vp}*, *parP_{Vp}*, or both resulted in 50-60% of cells having a reduction in either chemotaxis protein foci formation or polar localization (51). Through fluorescence microscopy, it was determined that ParC_{Pa} and ParP_{Pa} were required for optimal chemotaxis protein foci formation in *P. aeruginosa* (Figure 3.3). CheA-mTurquoise (mTq) expressed from the native site in the chromosome was used as a marker for chemotaxis protein foci formation and localization (84) as CheA, along with CheW and MCP, are required for higher order clustering (11). As a control, CheA foci formation was tested in the *cheW* mutant and showed a 96% reduction as previously published (77). CheA foci formation was reduced by ~45-50% in the *parC_{Pa}* and *parP_{Pa}* deletion mutants (Figure 3.3B). Surprisingly, in the *parC_{Pa}* and *parP_{Pa}* deletion strains, the polar localization of CheA foci remained largely unchanged compared to wild type. This suggests that the Par-like proteins are more important for foci stability or inheritance as opposed to localization. The three amino acid residues that are different between CheA from PAO1 and PA14 do not affect function as the *P. aeruginosa* PAO1 strain expressing CheA-mTq from PA14 was capable of wild type chemotaxis (Figure 3.4A) and therefore its use was justified for localization studies. The CheA-mTq fusion protein was present in all mutant backgrounds (Figure 3.4B), demonstrating that the lack of foci formation was not due to reduced levels of CheA. Curiously, western blotting suggested that CheA-mTq levels were slightly higher in the mutants compared to wild type. The reason for this increase in CheA levels remains to be determined.

3.3 ParP_{Pa} has a CheW-like domain

An alignment of ParP_{Pa} and CheW showed that the C-terminal half of ParP_{Pa} had homology to CheW (Figure 3.5A). This led us to speculate that these proteins may have functional redundancy. To test for this, a swimming assay was performed wherein CheW was expressed in $\Delta parP_{Pa}$, as well as the inverse combination (Figure 3.5B). Interestingly, expression of *his-cheW* partially complemented the *parP_{Pa}* mutant to the same degree as *his-parP_{Pa}*. However, *his-parP_{Pa}* could not complement the *cheW* mutant, which suggested that CheW has functional similarity to ParP_{Pa}. A western blot showed that His-ParP_{Pa} and His-CheW were both expressed in the mutant backgrounds without arabinose induction (0%) (Figure 3.6), which are the conditions used in the swimming assay in the preceding figure (Figure 3.5). It is also possible that deletion of *parP_{Pa}* resulted in polar effects on the expression of *cheW*. It is computationally predicted that the genes encoding ParP_{Pa} and CheW are in the same operon (120). This operon has genes encoding *parP_{Pa}*, *cheW* and PA1465 in this sequence. Therefore, gene fragments of *parP_{Pa}-cheW* and *cheW-PA1465* were amplified from the chromosome and cloned into the arabinose inducible expression vector pJN105. These constructs were then transformed into *parP_{Pa}* and *cheW* mutant backgrounds and used in a swimming motility assay, which showed that these two-gene inserts were better able to complement the single-gene inserts of *parP_{Pa}* or *cheW* (Figure 3.5B). These results suggested that co-expression of these proteins is important, although the exact cause for the increase in complementation has yet to be investigated.

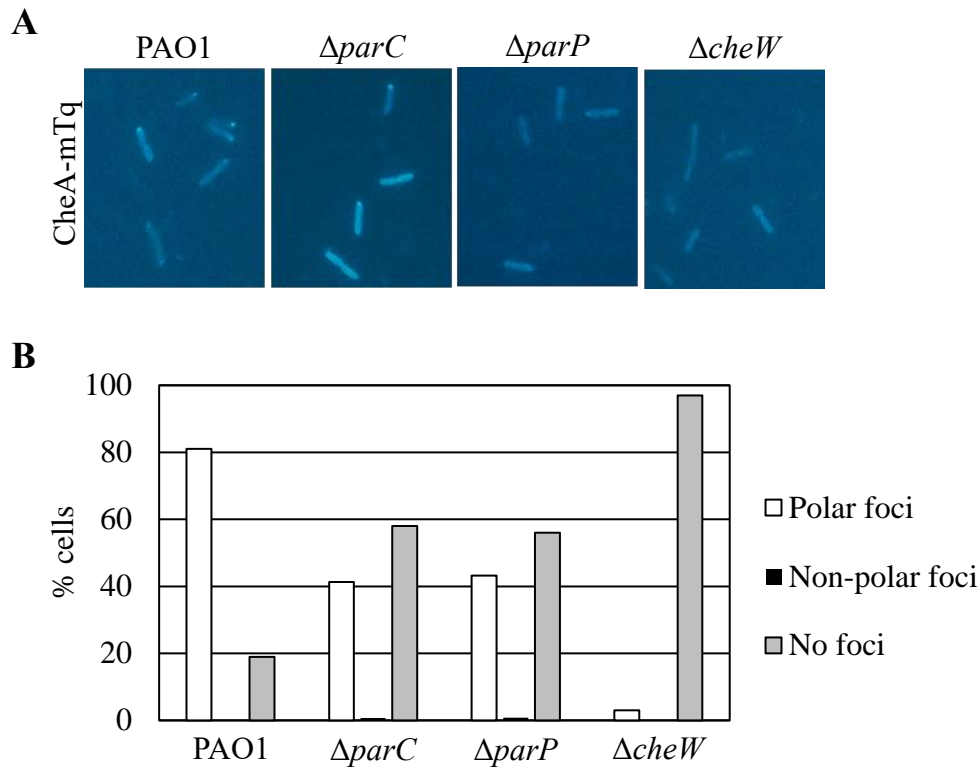


Figure 3.3 – The Par-like proteins affect chemotaxis protein localization. (A) Representative images of CheA-mTq foci formation in wild type and indicated mutant *P. aeruginosa* strains. (B) Quantitation of CheA-mTq foci formation and localization in mutant *P. aeruginosa* strains. 248 cells were counted.

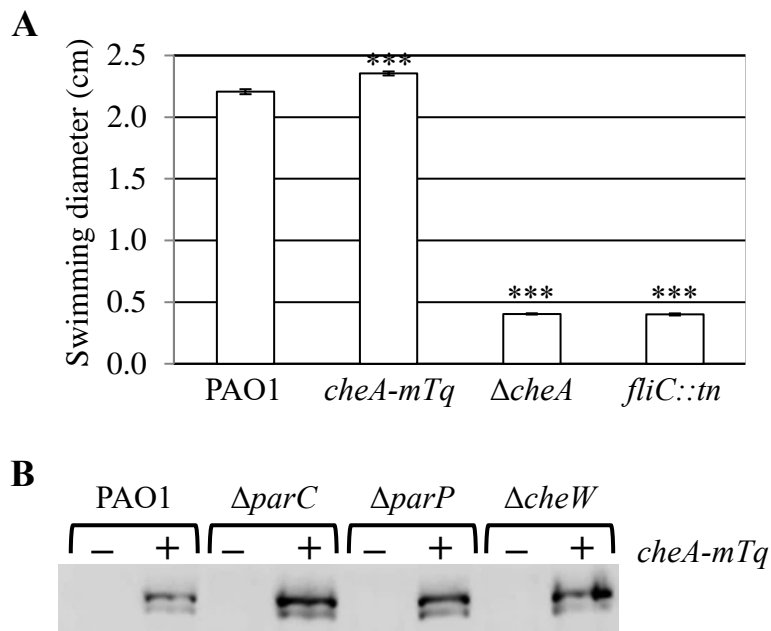


Figure 3.4 – CheA-mTq is functional and present at higher levels in the *par*-like mutants. (A) Swimming motility assay of wild type and indicated *P. aeruginosa* strains. The average swimming diameter measurements are shown and error bars denote the standard error of the mean. *** = $p < 0.0001$ compared to wild type. (B) Western blot showing CheA-mTq levels in the indicated strains.

A

```

ParPPa MSAATATRSQALALQSYLDALLQEATFEDLEPLVETPPAPAPAPLKPVALAVA EVATPAPA
CheW -----

ParPPa LETLPVDHGFDEFEEAAVLEEQRDARLVPPAPAALLDEPTTLREL PVEPRPHEVIELRVP
CheW -----MS
      :

ParPPa SAPASVGEPPLLDPLLLDDGRPAWAAEPFECLLFDVAGLT LAVPLVCLGSIYPLENQELT
CheW KATAQSAEDPIL-----QWVTF-----RLDNESYGINV--MQVQEV LRYTEIA
      . * * . * * : * * * * * : : : : : : * * : :

ParPPa PLFGQPDWFLGILPSQAGNLKVLDTARWMPERYRDDYRDGLKY-VISVQGYEWGLAVHQ
CheW PVPGAPSYVLGIINLRGNVVTVIDTRQRFGLDPAP--VSDNTRIVII EADKQVVGILVDS
      * : * * . : * * * : : . . : * * * * : . : * . : : * . : * : * .

ParPPa VSR S I R L D P A E V K W R S Q R S Q R P W L A G T V I E H M C A L - - - - L D V A A L A E L I A S G A V K R L H G D
CheW V A E V V Y L K Q S E I E T A P N V G N - - E E S A K F I Q G V C N K N G E L L I L V E L D K M M T E E E W S E L G S I
      * : . : * . : * : : : : : : : . . . . * : * * * * * * : . * * : : : . * .

ParPPa H
CheW -

```

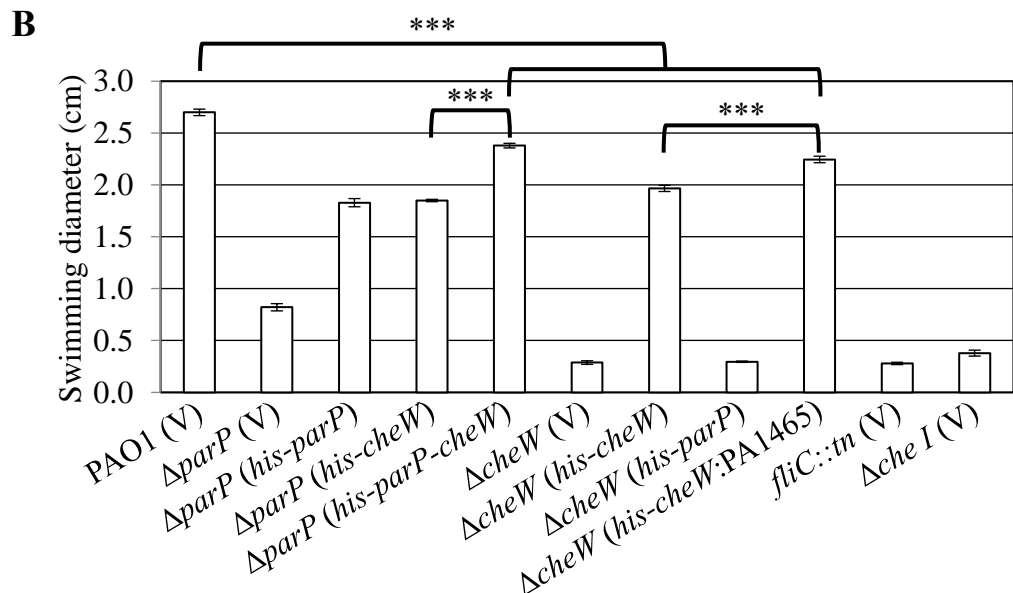


Figure 3.5 – CheW may have functional redundancy to the CheW-like domain of ParP. (A) Alignment of ParP and CheW using Clustal Omega; “*” means identical, “:” means high similarity and “.” means low similarity of the amino acid residues. (B) Swimming motility assay of wild type and indicated *P. aeruginosa* strains without arabinose induction. The average swimming diameter measurements are shown and error bars denote the standard error of the mean. *** = $p < 0.0001$ compared to wild type.

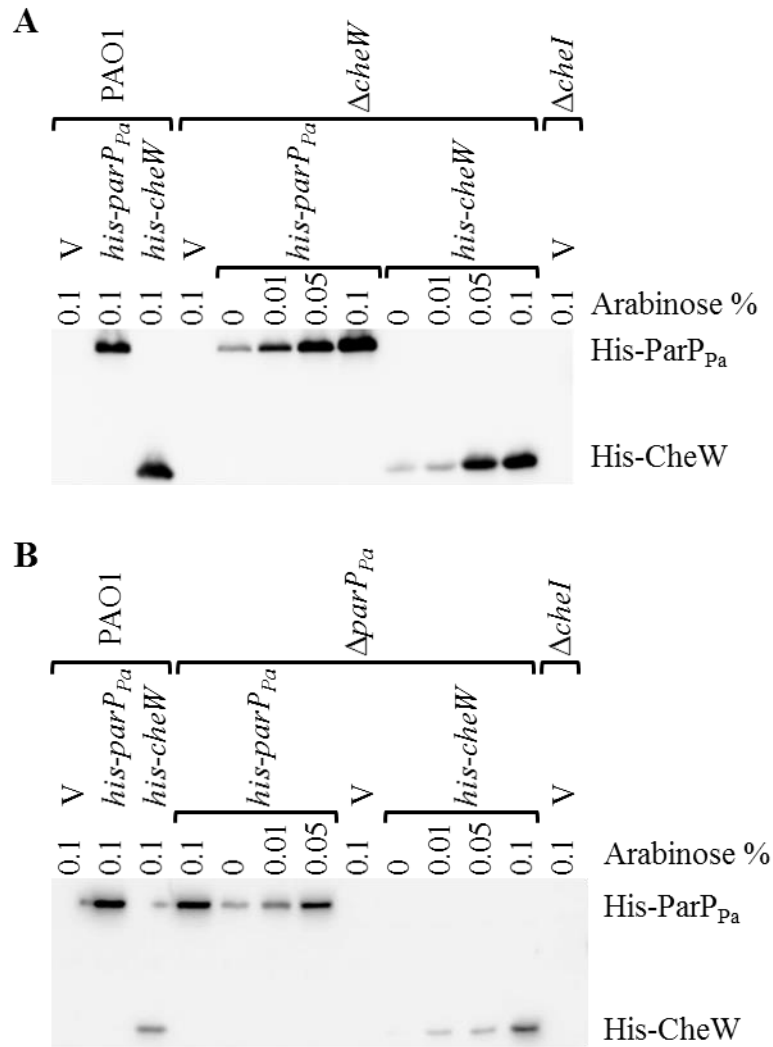


Figure 3.6 – Induction of His-ParP_{Pa} and His-CheW results in expression. Western blots showing His-ParP_{Pa} and His-CheW levels in (A) *cheW* and (B) *parP_{Pa}* mutants.

3.4 DipA interacts with ParP_{Pa} and affects swimming motility and surface flagellin levels

Because deletion of the *par*-like genes affected swimming motility and chemotaxis protein foci formation, and the classical Par proteins, ParA and ParB, have been shown to interact with each other, it was proposed that ParC_{Pa} and ParP_{Pa} may interact directly with each other, the chemotaxis proteins and MCPs. Given that the genome of *P. aeruginosa* is reported to encode 26 MCPs, a select number of representative MCPs were assayed for interaction with the Par-like proteins. The MCPs chosen were PA1930 (McpS), PA2867 and PA4290. McpS is involved in chemotaxis and is like TlpT from *R. sphaeroides* in that it is a soluble chemoreceptor (7, 78). PA2867 and PA4290 both have short periplasmic sensing domains and it was therefore thought that these MCPs may not be sensing ligand but instead could have additional roles in the cell. In *V. parahaemolyticus*, ParC_{Vp} and ParP_{Vp} interact directly with each other and CheA (51). A bacterial two-hybrid (B2H) assay showed that ParC_{Pa} and ParP_{Pa} directly and strongly interact with each other and weakly interact with CheA and the MCPs (Figure 3.7). ParC_{Pa} could self-interact, thus further suggesting that it is acting as a ParA-like protein (51, 121). It was reported by Kulasekara *et al* (2013), that in *P. aeruginosa* strain PA14, CheA co-immunoprecipitated with the phosphodiesterase Pch (PAO1 annotation: PA5017; hereafter referred to as DipA for clarity within the literature). This indicated that CheA and DipA form a complex with each other, but it was not known if this interaction was direct or indirect. DipA is known to be involved in biofilm dispersion and swimming motility and its ability to form polar protein foci is dependent on CheA (84, 111). Because the Par-like proteins affect CheA foci formation and swimming motility, DipA and the Par proteins were assayed for direct interactions. Strikingly, a B2H assay revealed that ParP_{Pa} directly and strongly interacts with DipA (Figure 3.7). No direct interaction could be detected between DipA and CheA using this assay, however, this result is inconclusive as DipA

does not appear to be functional when expressed from pBT in other B2H assays (data not shown). The negative controls used in this assay were empty pBT and pTRG together, or empty vector with a gene of interest on the other vector. These combinations were used to determine if interactions seen between two test proteins could have been the result of a test protein interacting with vector-based λ cI or RNA polymerase α subunit from pBT and pTRG, respectively. The negative controls with a gene of interest occasionally had growth on dual selective media, and the controls which had the most growth were then compared to their corresponding test interactions. In this case, the growth of the negative control was subtracted from the growth of test interaction to get the net strength of the interaction. If the result of this subtraction was zero or a negative number, then that was interpreted as no interaction. The positive control used was *lgf2*:pBT and *gallI*:pTRG and this represents a very strong interaction, which results in equal growth on both the nonselective and dual selective media.

The *dipA* mutant showed a 63% reduction in swimming motility, which is similar to the *parP_{Pa}* mutant, which had a 70% reduction in swimming motility, yet these results were significantly different from each other (Figure 3.8A). Complementation with His-DipA fully restored swimming motility to the *dipA* mutant (Figure 3.8A). Western blots confirmed that both His-DipA and His-ParP_{Pa} were expressed (Figures 3.8B and 3.6B).

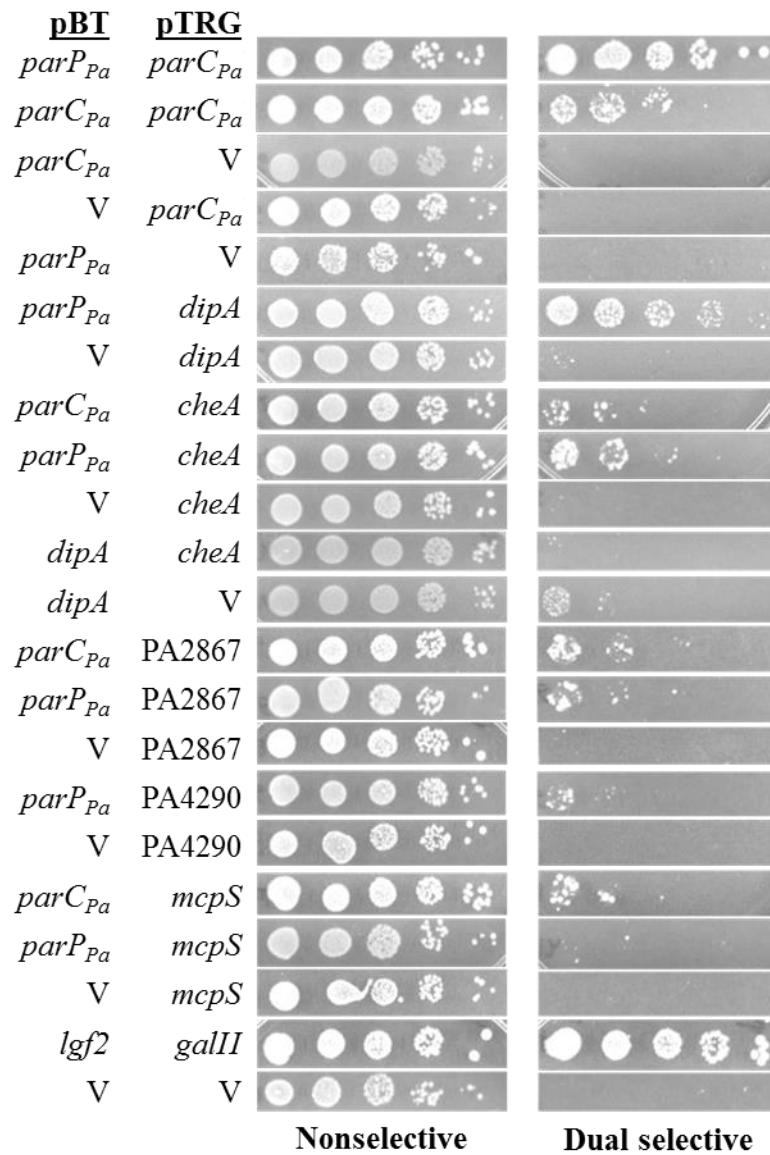


Figure 3.7 – DipA interacts directly with ParP_{Pa}, as demonstrated by a bacterial two-hybrid assay. 5 µl of a 10-fold dilution series are spotted from left to right. Cultures on the nonselective media function as a loading control, while dual selective media reveals the strength of the protein-protein interactions. Strong interactions have growth to the right-most spot, as indicated by the positive control *lgf2* and *gallI*.

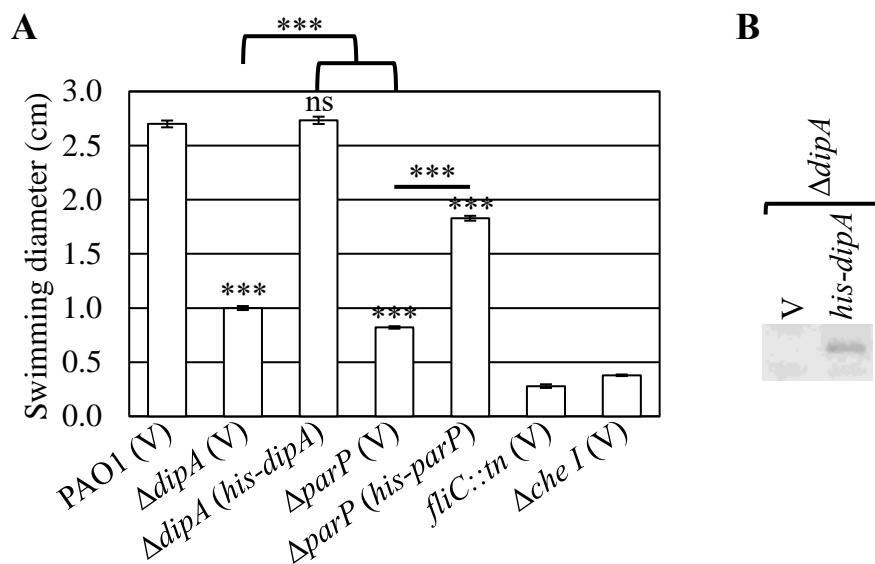


Figure 3.8 – Deletion of DipA results in a similar reduction of swimming motility as seen in $\Delta parP$. (A) Swimming motility assay of indicated *P. aeruginosa* strains. The averaged swimming diameters are shown and error bars denote standard error of the mean. *** = $p < 0.0001$ compared to wild type and ns = not significant. (B) Western blot showing His-DipA levels.

To determine if the cause of the swimming motility defects was strictly due to a loss of chemotaxis foci formation in the *par*-like mutants, the amount of surface flagellin in the *parC_{Pa}*, *parP_{Pa}* and *dipA* mutant cells was quantified. Surface flagellin levels were increased in the *parP_{Pa}* and *dipA* mutants (Figure 3.9). Using ImageJ software to determine relative protein levels, a ~15% increase in surface flagellin levels was found in the *parP_{Pa}* mutant compared to wild type. The relative protein levels of the *dipA* mutant were not calculated. Flagellin is encoded by *fliC* and is the subunit of the flagellum; the *fliC* transposon mutant functioned as a negative control in this assay. A limitation of this assay is that it does not reveal if the increase in surface flagellin levels is due to increased flagellation or longer flagella. We are currently unable to distinguish between these possibilities, as flagellar staining of these strains yielded inconsistent results (data not shown).

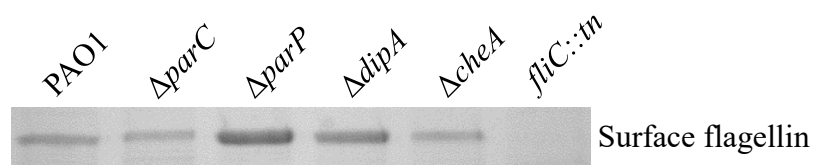


Figure 3.9 – Deletion of *parP* and *dipA* increases surface flagellin levels. Surface flagellin levels in wild type and mutant *P. aeruginosa* strains.

3.5 DipA, ParP_{Pa} and CheA polar localization is interdependent

Localization dependence of CheA, DipA and ParP_{Pa} was determined by fluorescence microscopy. CheA-mTq foci formation or localization remained unchanged in a *dipA* mutant, indicating that CheA localization is independent of DipA (Figure 3.10A and B). Levels of CheA-mTq protein remained unchanged in the *dipA* mutant (Figure 3.10C). ParP_{Pa} foci formation was reduced by 50% in a *dipA* mutant and 60% in a *cheA* mutant, but there was no change in localization (Figure 3.11A and B). DipA foci formation was reduced by 50% in a *parP_{Pa}* mutant and 95% in a *cheA* mutant (Figure 3.12A and B). The dependence of DipA on CheA for foci formation has been previously published (84). Expression of the ParP and DipA fluorescent fusion proteins complemented the swimming defect of their respective mutant parent strains to the same levels as the His-tagged ParP and DipA proteins (data not shown), thereby demonstrating that these fusion proteins are as functional as the His-tagged versions (Figure 3.13). DipA fusion protein was present at similar levels in all mutant backgrounds, demonstrating that a loss of foci formation was not due to protein instability or low expression levels (Figure 3.12C). The levels of ParP fusion protein in $\Delta parP\Delta cheA$ and $\Delta parP\Delta dipA$ appeared less than in $\Delta parP$ (Figure 3.11C). However, a previous western blot showed that ParP fusion protein levels were very similar between wild type and the *dipA* mutant (data not shown), indicating that additional testing is needed to confirm Yfp-ParP levels in these strains. The results of fluorescence microscopy of ParC, ParP, CheA and DipA localization show that there is an interdependence on localization, particularly for ParP on CheA and DipA, DipA on ParP, and CheA on ParP (Figure 3.14).

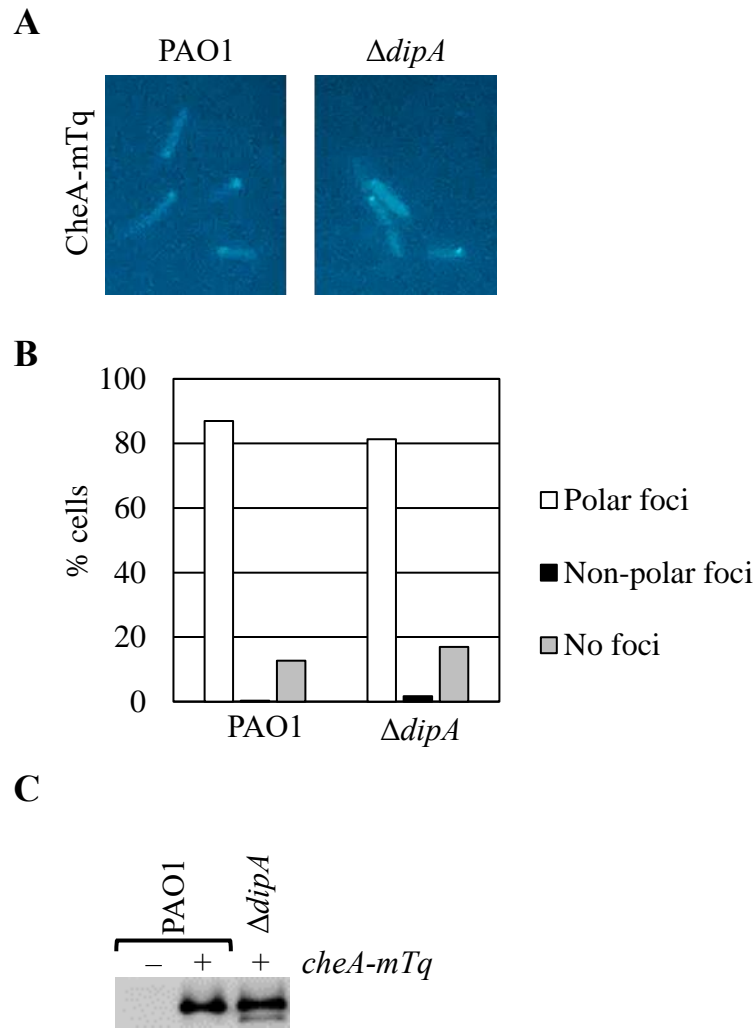


Figure 3.10 – DipA is not required for CheA foci formation or localization. (A) Representative images of CheA-mTq foci formation in wild type and mutant *P. aeruginosa* strains. (B) Quantitation of CheA-mTq foci formation and localization in the indicated *P. aeruginosa* strains. 300 cells were counted. (C) Western blot showing CheA-mTq levels.

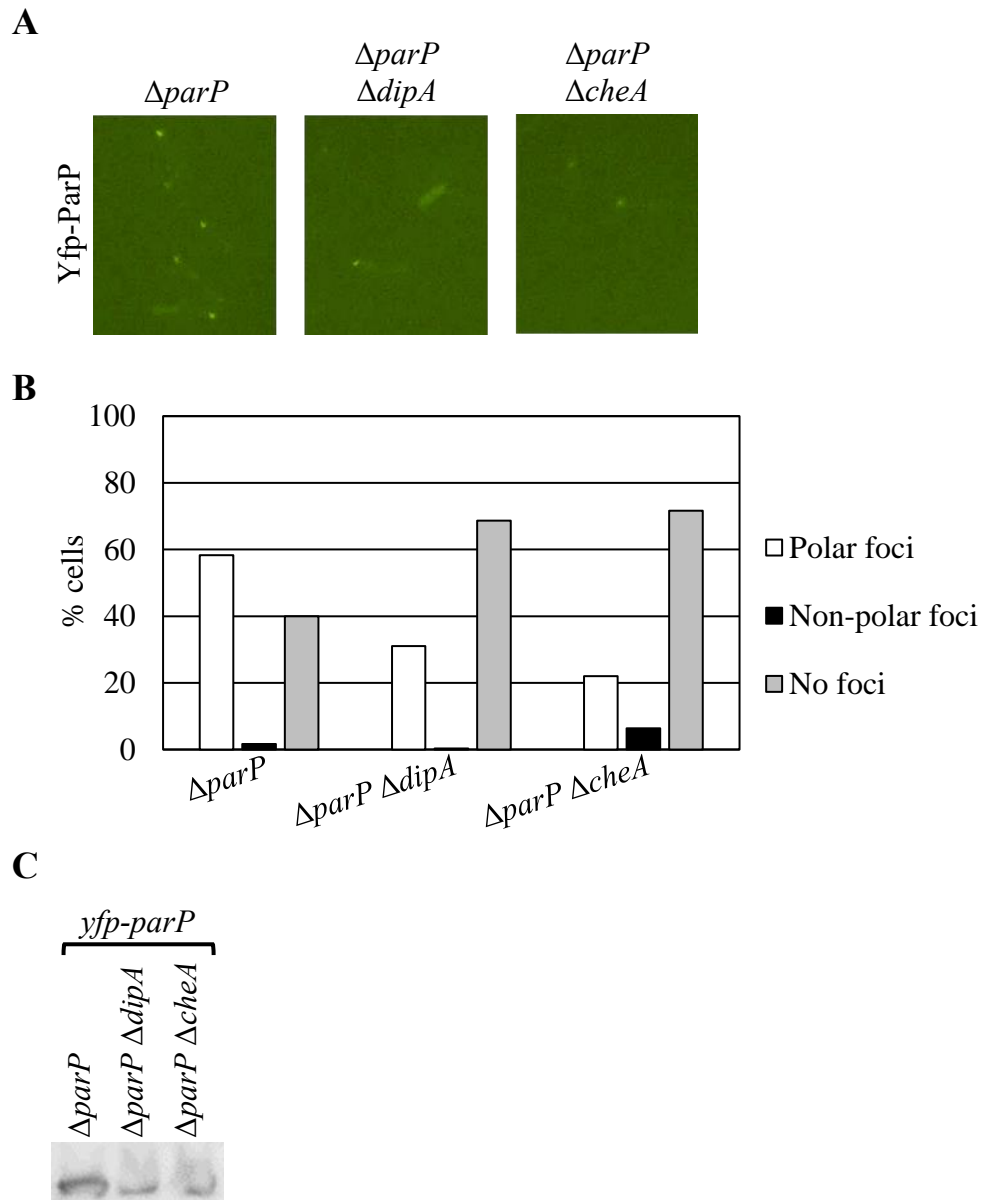


Figure 3.11 – ParP foci formation is dependent on DipA and CheA. (A) Representative images of Yfp-ParP foci formation in wild type and mutant *P. aeruginosa* strains. (B) Quantitation of Yfp-ParP foci formation and localization patterns in the indicated *P. aeruginosa* strains. 300 cells were counted. (C) Western blot showing Yfp-ParP levels.

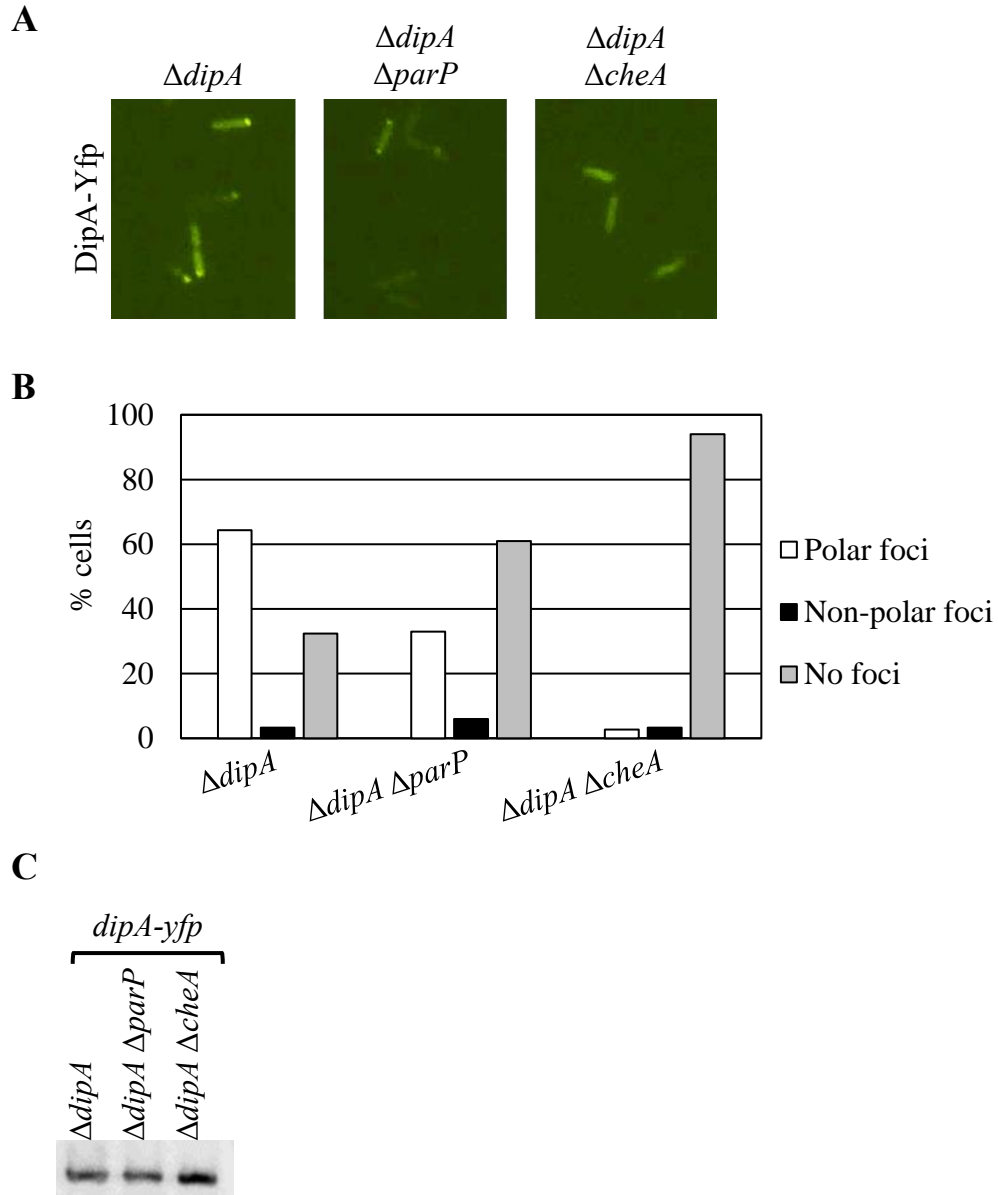


Figure 3.12 – DipA foci formation is dependent on ParP and CheA. (A) Representative images of DipA-Yfp foci formation in wild type and mutant *P. aeruginosa* strains. (B) DipA-Yfp foci formation and localization patterns in the indicated *P. aeruginosa* strains. 300 cells were counted. (C) Western blot showing DipA-Yfp levels.

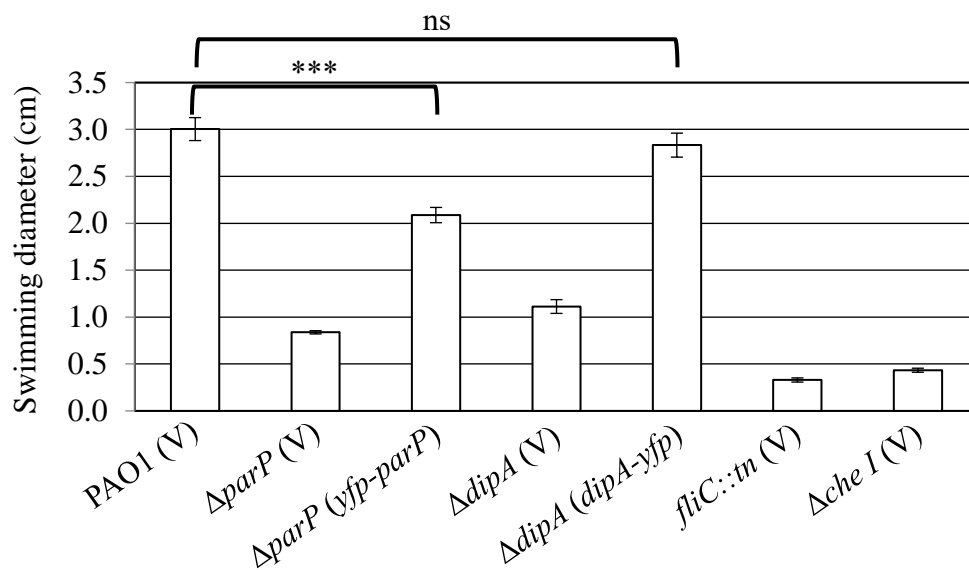


Figure 3.13 – Fluorescent fusion proteins Yfp-ParP and DipA-Yfp are functional. (A) Swimming motility assay of wild type and indicated *P. aeruginosa* strains. The average swimming diameter measurements are shown and error bars denote the standard error of the mean. *** = $p < 0.0001$ compared to wild type and ns = not significant.

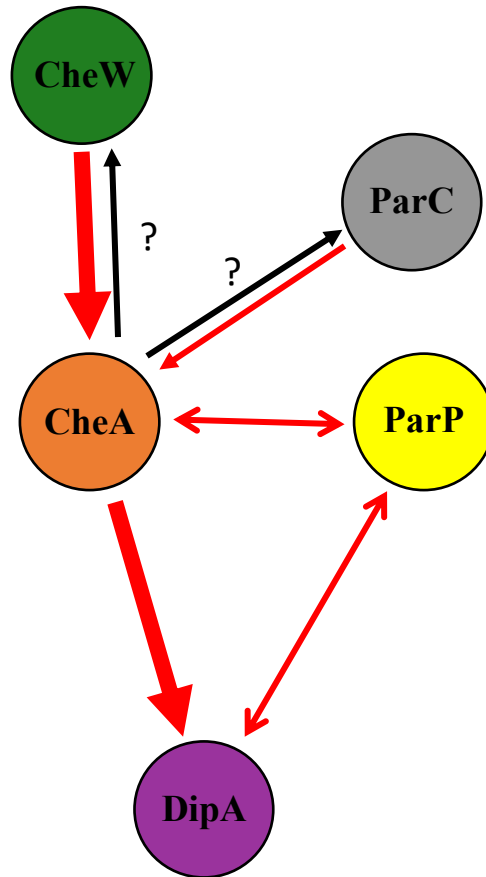


Figure 3.14 – Model showing the dependence on foci formation between the Par-like proteins and the chemotaxis and biofilm dispersion systems of *P. aeruginosa*. The red lines indicate that the absence of one protein will lead to loss of foci formation of another protein, as shown by an arrowhead. A line with two arrowheads indicates interdependence on localization. The thickness of the arrow represents the effect of foci loss. Black arrows mean that the localization dependence was not tested.

3.6 ParC has a conserved ATPase domain which may be important for swimming motility

A protein alignment of ParC_{Pa} along with representative ParA partitioning protein types Ia, Ib, and II showed that ParC_{Pa} is similar to type Ib proteins as it lacks the N-terminal regulatory region that is present in type Ia and it has a conserved ATPase domain (Figure 3.15). The conserved ATP binding and ATP hydrolysis domains seen in PpfA and ParC_{Vc} have homology with the ATPase domain of ParC_{Pa} (Figure 3.16) (7, 48).

A point mutation in the predicted ATP binding site of the ATPase region of *parC_{Pa}* was made (*parC_{Pa}-K15A*) and this construct was expressed from pJN105. When *parC_{Pa}-K15A* was expressed in Δ *parC_{Pa}*, there was a statistically significant decrease in swimming motility compared to Δ *parC_{Pa}* with empty vector (Figure 3.17). This contrasts with the partial complementation that was seen with wild type *parC_{Pa}* expression in the same mutant (Figure 3.17). This suggests that the conserved ATPase domain is required for ParC_{Pa} function and that the loss of the putative ATP binding site has a dominant negative effect on the basal level of swimming compared with wild type ParC_{Pa}. This negative effect was also seen when ParC_{Pa}-K15A was expressed in the wild type strain. However, since overexpression of ParC_{Pa} has previously been shown to negatively impact swimming motility (data not shown), it remains necessary to quantify the relative levels of ParC_{Pa}-K15A expression to determine if this phenotype is due to over-expression or the K15A mutation. Protein levels of the wild type and mutant ParC_{Pa} have not been determined. As such, the possibility of uneven levels of protein expression influencing these results remains a distinct possibility.

```

ParM (II) -----MLVFIDDGS--TNIKLRWQENDGTIKQ-----
SopA (Ia) MFRMRLMETLNQCINAGHEMTKAI AIAQFNDDSP EARKITRRWRIGEAADLVGVSSQAIR
Soj (Ib) -----
ParCPa -----

ParM (II) -----HISPNSFKREWAVSFGDKK
SopA (Ia) DAEKAGRLPHPDMEIRGRVEQRVGYTIEQINHMRDVFGTRLRRAEDVFPPVIGVAAHKGG
Soj (Ib) -----MGKIIAITNQKGG
ParCPa -----MKVWAVANQKGG
                                                                . : : .

ParM (II) VFNYT-----LNGEQ-YSFDPI SPDAVVTTNIAWQYSDVNVVAV----HHALLTS
SopA (Ia) VYKTSVSVHLAQDLALKGLRVLLVEGNDPQGTASMYHGWVPDLHIHAEDTLLPFYLGEKD
Soj (Ib) VGKTTT SVNLGACLAYIGKR VLLVD-IDPQGNAT SGLGIEKADVDHC VYDILVDDADVTD
ParCPa VGKTTSSIALAGLLADAGKR VVVVD-LDPHGSMT SYFGYDPDTLEHS AFDFLFLHQGNVPE
* : : * : . : . * . : . .

ParM (II) GLPVSEVDIVCTLPLTEYYDRNNQPNTENIERKKANFRKKITLNGGDTFTIKDVKVPES
SopA (Ia) -DVTYAIKPTCWP-----GLDIIP SCLALHRIETELMGKFDEGKLP TDPHMLRLAIET
Soj (Ib) I-----IKPTSVE-----NLDVIPATIQLAGAEIELVPTISRE-----VRLKRALES
ParCPa GLPASLLRSTSNE-----RISLLPSSTALATLERQSPGKSGLG-----LVVSKSLAQ
: . . . * : : : . :

ParM (II) IPAGYEV LQELDELDSLIIIDLGTTLDISQVMGKLSGISKIYGDSSLG VSLVTSAVKD-
SopA (Ia) VAHDYDV-----IVI-----DSAPNLGIGTINVVCAAD
Soj (Ib) VKQNYDY-----MII-----DCPPSLGLLTINALTASD
ParCPa LWQDFDH-----AII-----DSPPLLGVLMVNALAASQ
: : : : * : : : ** : .

ParM (II) AL-----SLARTKGSSYLADDII---IHRKDNNYL-----KQRINDENKISIVTEAM
SopA (Ia) VLIVPTPAELFDYTSALQFFDMLRDLKKNVDLKGFE PDVRI LLTKYSNSNG---SQSPWM
Soj (Ib) SVVIPVQCEYYALEGLS QLLNTVRLVQKHLNT--DLMIEGVLLTMLDARTNLGIQVIEEV
ParCPa HLVIPVQTEFLAVKGLERMVNTLAMINRSRKQ--ALP-YTIVPTLFD RRTQASLSTLRIL
: . . : : : . . :

ParM (II) NEALRK-LEQRVLNT---LNEF--SG-----YTHVMVIGGGAELIC
SopA (Ia) EEQIR-DAWGSMVLKNV-VRETDEVG-----KGQIRMRTVFEQAIDQRSSTGAWR
Soj (Ib) KKYFRDKVYQTII PRNVRLSEAPSHGKPI ILYDPRSRGAEVYLDLAKEVAANG-----
ParCPa NENYPDNLWQAFIPI DTRLRDASRAGVTPSQHDGKSRGVIA YRALLKHL LAQQPATRVA-
: : . : : * .

ParM (II) DAVKKHTQIRDERFFKTNNSQYDLVNGMYLIGN
SopA (Ia) NALSIWEPVCNEIFDRLIKPRWEIR-----
Soj (Ib) -----
ParCPa -----

```

Figure 3.15 – Alignment of the amino acid sequences of ParA type Ia, Ib, and II proteins along with ParC_{Pa} for comparison. Clustal Omega was used for this alignment; “*” means identical, “:” means high similarity and “.” means low similarity of the amino acid residues. The green highlighted region is the ATPase domain of Soj. The text within the parentheses indicates the ParA protein type.

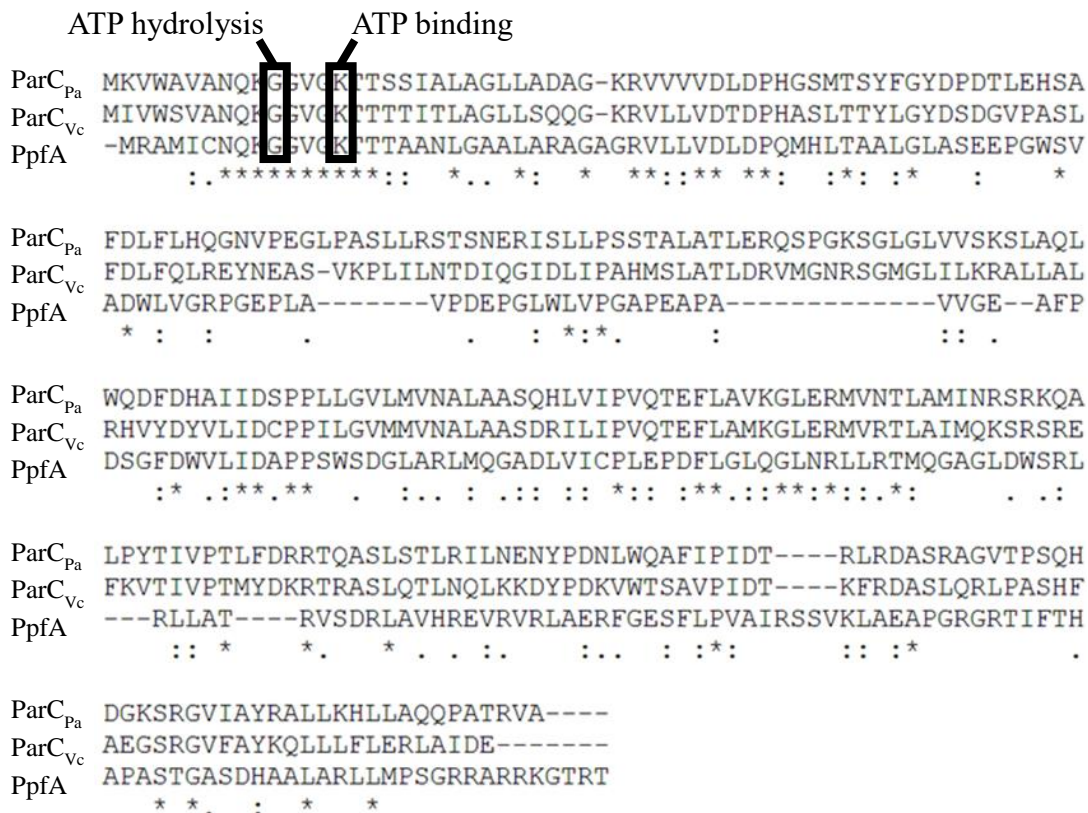


Figure 3.16 – Alignment of the amino acid sequences of ParC_{Pa}, ParC_{Vc}, and PpfA. Clustal Omega was used for this alignment; “*” means identical, “:” means high similarity and “.” means low similarity of the amino acid residues. Labeled are amino acid residues that are important for ATP binding and ATP hydrolysis in ParC_{Vc} and PpfA.

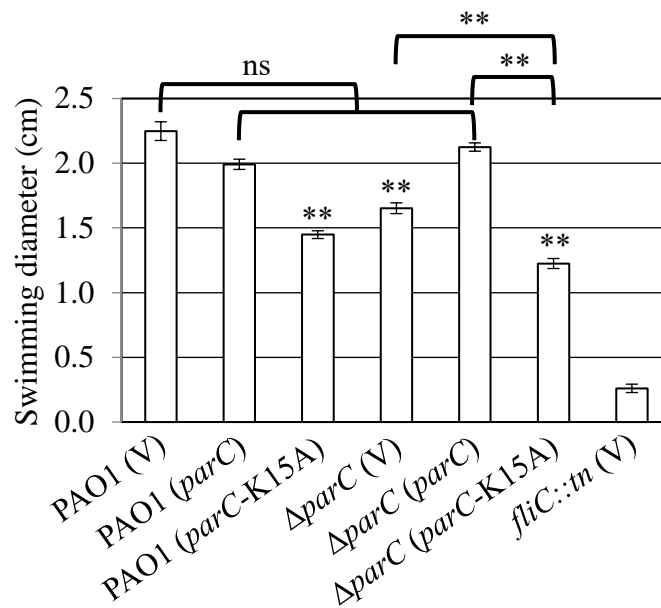


Figure 3.17 – Mutation of the proposed ATP binding site has a dominant negative effect on swimming motility compared with wild type ParC. Swimming motility assay of indicated *P. aeruginosa* strains complemented with wild type ParC or ParC-K15A. The average swimming diameters are shown and error bars denote standard error of the mean. ** = $p < 0.001$ compared to wild type and ns, not significant.

Chapter Four

Discussion

Chemotaxis proteins localize to distinct regions within a bacterial cell – this localization can vary depending on if it is a random or ordered process. In *E. coli*, they localize to the poles as large clusters, yet small clusters and individual proteins can be seen at the lateral regions of the inner membrane (53). The mechanism by which this occurs is believed to be stochastic, as *E. coli* does not have *par*-like genes encoded within its chemotaxis gene cluster (47). Instead, individual MCPs are inserted randomly into the membrane, where they can nucleate a new cluster or join an existing one. Other organisms, such as *Vibrio* spp. and *R. sphaeroides*, have *par*-like genes in their chemotaxis gene clusters and the encoded proteins are used for chemotaxis protein cluster formation and localization (7, 48, 51). *P. aeruginosa* has *par*-like genes encoded in its main chemotaxis gene cluster, *che I* (Figure 3.1A), and this work provides convincing evidence that these Par-like proteins are involved in chemotaxis and linked to DipA, a phosphodiesterase involved in biofilm dispersion.

Previous studies in *Vibrio* spp. and *R. sphaeroides* have shown that the conserved ATPase domain of ParA-like proteins is needed for proper partitioning and localization of chemotaxis protein clusters (7, 48, 51). The residues for ATP hydrolysis and ATP binding in PpfA are required for cytoplasmic chemotaxis cluster formation in *R. sphaeroides*. In *V. cholerae* ParC_{Vc}, ATP binding is needed for cluster formation and ATP hydrolysis is necessary for the polar localization of these clusters (48). In *V. parahaemolyticus*, the ability of ParC_{Vp} to bind or hydrolyze ATP is needed for proper chemotaxis protein cluster formation and localization, and for interaction with ParP_{Vp} and CheA (51). The defect in chemotaxis protein clustering is approximately the same in the *parC_{Vp}* deletion strain and the ATP binding mutant *parC_{Vp}-K15A*, suggesting that the defect in the *parC_{Vp}* mutant is via a defect in ATP binding. Our work shows that mutation of the putative ATP binding residue of ParC_{Pa} may result in a dominant negative

swimming phenotype, compared with expression of wild type ParC_{Pa} in PAO1 cells (Figure 3.17). Further testing needs to be done to confirm these results, and to determine the effect this mutation has on the localization of ParC_{Pa}, and its interactions with ParP_{Pa} and chemotaxis proteins.

The Par-like proteins are known to be involved in swimming motility in *Vibrio* spp. and swarming motility in *R. sphaeroides* (48, 51, 63). Our work shows that in *P. aeruginosa*, ParC_{Pa} and ParP_{Pa} are needed for optimal swimming motility (Figure 3.1B). Comparison of the phenotypes between *V. parahaemolyticus* and *P. aeruginosa* reveal that the *parP_{Vp}* mutant has a swimming defect equal to that of the *parC_{Vp}* mutant. However, ParP_{Pa} is distinct in that it appears to have a more significant role in swimming motility than ParC_{Pa}, and possible reasons for this will be discussed below.

Alignment of all ParP proteins show that their C-terminal halves are all homologous to CheW (51). The homologous CheW-like domain in ParP_{Vp} was shown to be required for direct interactions with CheA in *V. parahaemolyticus*. Our results show that in terms of swimming motility, CheW can complement a *parP_{Pa}* mutant just as well as ParP_{Pa}, but ParP_{Pa} cannot complement a *cheW* mutant (Figure 3.5B). It remains unclear whether these results are real or due to resolution of polar effects on CheW expression. It is possible that the inability of ParP_{Pa} to complement CheW is due to the presence of the additional N-terminal domain found in ParP_{Pa} (Figure 3.5A). This N-terminal domain could prevent the CheW-like domain of ParP_{Pa} from interacting with the MCP hairpin tip, within the signaling region, and the CheA P5 domain where CheW normally binds. To test this possibility a truncated ParP_{Pa} lacking the N-terminal domain could be expressed in the *cheW* mutant to determine if complementation occurs. The presence of the CheW-like domain also suggests that ParP_{Pa} may function as a lesser adaptor

protein, holding certain MCPs in a polar cluster. Because CheW can complement ParP_{Pa}, this could indicate functional redundancy between these proteins.

The Par-like proteins are known to dimerize and interact with each other and with the chemotaxis system via CheA in *V. parahaemolyticus* (51). Our work confirms that ParC_{Pa} can dimerize and strongly interact with ParP_{Pa}, and both proteins interact with CheA (Figure 3.7). We did not observe ParP_{Pa} self-interaction (data not shown). It was determined that the Par-like proteins of *P. aeruginosa* interacted with representative MCPs, thus demonstrating that ParC_{Pa} and ParP_{Pa} are not linked to the chemotaxis system only via CheA. Strikingly, we found that ParP_{Pa} interacted strongly with DipA (Figure 3.7). These results are novel, as ParP_{Pa} and DipA form the first direct link between the biofilm dispersion and chemotaxis systems. It was previously shown by co-immunoprecipitation that DipA and CheA form a complex, but it was not known if this was through direct or indirect interactions (84).

The *dipA* mutant had a reduction in swimming motility that was similar, but significantly different to what was seen in the *parP_{Pa}* mutant (Figure 3.8A). Reductions in swimming motility can be due to alterations in chemotaxis, flagellation or flagellar function, so we performed additional testing to ascertain the mechanism(s) behind the $\Delta parP_{Pa}$ and $\Delta dipA$ reduction in swimming motility. It was determined that *parP_{Pa}* and *dipA* mutants have slightly increased levels of surface flagellin (Figure 3.9). This may be due to increased flagellar length or the presence of multiple flagella. Initial studies were inconclusive, and as such the reason for the increase in surface flagellin levels in the *par*-like mutants of *P. aeruginosa* remains unknown. In *V. cholerae*, the absence of HubP results in a small subset of cells (6%) having multiple polar flagella compared with wild type (1%) (61). HubP is a polar-organizing protein and its obvious homolog is FimV from *P. aeruginosa*. While FimV is polarly-localized, it is reported to function

in the localization of twitching motility proteins (122). To date, FimV has not been shown to be involved in chemotaxis or flagellar-based motility.

In *P. aeruginosa* PA14, Kulasekara *et al* (2013) showed that loss of DipA (referred to as Pch in their publication) leads to a loss of c-di-GMP heterogeneity in individual cells, with most cells having high levels of c-di-GMP. A reduction in flagellar reversals and average cell velocity compared with wild type was also observed. These results suggest that c-di-GMP levels modulate flagellar reversals and cell velocity, however, the mechanism by which this occurs has not been determined but may involve a c-di-GMP effector protein. DipA forms polar foci at the flagellated pole with CheA. After cell division, one of the daughter cells will inherit the flagellum and a DipA cluster, which lowers the c-di-GMP levels in that cell, thus creating c-di-GMP heterogeneity in individual cells. The role of this heterogeneity is speculated to give a survival advantage to these cells in unpredictable environments (84). Individual cells with high or low c-di-GMP levels would likely tend to either attach to a surface and start biofilm formation or remain motile and spread to new areas. In this sense, at any moment, there are cells that are “primed” for either choice, depending on the environment. The presence of CheA is absolutely required for DipA polar localization and the phosphorylation activity of CheA promotes DipA PDE activity. The GTPase FlhF is required for polar localization of the flagellum, and in an *flhF* mutant, the flagellum is still produced but mislocalized from the pole (123). This results in cells having reduced swimming and swarming motility. Loss of FlhF also results in a reduction of transcription of class II, III or IV flagellar genes (123). This leads to reduced levels of *fliC* transcription and surface flagellin, which contrasts with the increased surface flagellin levels seen in the *parP* and *dipA* mutants (Figure 3.9). FlhF is above CheA and DipA in terms of dictating polar localization, but not their association with each other (84). The absence of FlhF

results in the mislocalization of the flagellum, and CheA and DipA foci from the pole. This suggests that the flagellum, CheA and DipA form a complex at one pole of the cell. However, it is not known if these three components remain in a complex when they are mislocalized from the pole. By forming these protein complexes, new daughter cells will be more likely to inherit necessary chemotaxis proteins to be used right away or once they synthesize a new flagellum.

Using fluorescence microscopy, we tested the chemotaxis system protein localization in the absence of the Par-like proteins. Deletion of either ParC_{Pa}, ParP_{Pa} or CheW resulted in a loss of CheA cluster, or foci, formation, but not polar localization in *P. aeruginosa* (Figure 3.3). Comparable results were seen for the Par-like proteins in *V. parahaemolyticus*, except that of the cells that had aberrant clustering, 50% of them had no clusters while the other 50% had non-polar clusters (51). These results suggest that in *P. aeruginosa*, the Par-like proteins function more in cluster stability as opposed to localization. Our results for the loss of CheA cluster formation in a *cheW* mutant agree with previously published work (77). Interestingly, we show that the loss in CheA cluster formation also coincided with a slight increase in CheA levels in the cells (Figure 3.4B). The absolute levels of MCP, CheW and CheA proteins can vary in a bacterium, but their stoichiometry appears to remain constant (2, 42). Overexpression of a chemotaxis protein can reduce chemotaxis and cluster formation (41, 42). One possible explanation for the reduction in CheA cluster formation in *P. aeruginosa* is that excess levels of CheA are present in the cell relative to the MCP and CheW proteins. However, our results do not show if the stoichiometry of MCP:CheW:CheA was altered - this would require further investigation.

The Par-like proteins are interdependent in their polar cluster formation. ParC_{Vp} and ParP_{Vp} are both needed for their cluster formation and polar localization in *V. parahaemolyticus*

(51). While we have not tested the interdependence of ParC_{Pa} and ParP_{Pa}, our work has shown that the clustering ability of ParP_{Pa} is interdependent on both CheA and DipA and that loss of cluster formation is ~50% (Figures 3.11A and B and 3.12A and B). These results suggest that the interdependence of localization between these proteins are equally important in their cluster formation. In a previous study and in this work, DipA cluster formation requires CheA (84). However, we found that CheA cluster formation and cellular levels are not dependent on DipA (Figure 3.10).

In summary, this work showed that the Par-like proteins of *P. aeruginosa* PAO1 are involved in chemotaxis controlling swimming motility. Our results correlate well with other studies in terms of the effects of the Par-like proteins on swimming motility and chemotaxis protein foci formation. Notably, we found that ParP_{Pa} plays a more significant role in swimming motility than ParC_{Pa}. We discovered that the c-di-GMP phosphodiesterase DipA interacts with ParP_{Pa} and that they have an interdependence in their cluster formation. Both the *parP_{Pa}* and *dipA* mutants have increased levels of surface flagellin. These results suggest that ParP_{Pa} and DipA work in the same pathway, and this may be the mechanism behind the large decrease in swimming motility in a *parP* mutant. We have provided compelling evidence that the chemotaxis and biofilm dispersion systems are linked together via DipA and ParP_{Pa} (Figure 4.1). When biofilm cells sense a nutrient cue to disperse, *dipA*, motility, and chemotaxis genes are upregulated, c-di-GMP levels decrease, the extracellular matrix is broken down, and cell adhesiveness is reduced (95, 111). Due to this series of events, cells become motile and chemotactic, and leave the biofilm. This leads to the question of what role ParP_{Pa} has in this process of dispersion and if DipA proteins can temporally, and perhaps spatially, switch between interactions with biofilm dispersal proteins and chemotaxis proteins, or if there are functionally

separate pools of this protein within the cell. Future studies could determine in more detail how loss of ParP_{Pa} has a greater defect in swimming motility than the loss of ParC_{Pa}. This could be addressed with follow-up experiments to the surface flagellin assay and CheA fluorescence microscopy and western blot data. Expression levels of *fliC* may be determined by quantitative RT-PCR, intracellular levels of FliC can be detected by western blot, and cell flagellation can be observed by fluorescent staining or transmission electron microscopy of the wild type and *parP_{Pa}* and *dipA* mutants and this would show how surface flagellin levels are increased. A promoter assay would show if *cheA* transcription is increased in the mutant strains, and if this is also seen in *parC* and *cheW* mutants. Fluorescence microscopy and a western blot of Δ *parP_{Pa}* and Δ *dipA* strains with fluorescently-tagged MCP, CheA and CheW would show if CheA levels alone are increased, shifting stoichiometry and inhibiting cluster formation, and if all tagged proteins have loss of foci formation in the mutant backgrounds. A swimming assay of a double deletion mutant of *parP_{Pa}* and *dipA* could be performed and if it results in a swimming defect approximately equal to the individual deletion mutants, then this would further confirm these proteins work together in chemotaxis. Long-term studies would include determining if ParP_{Pa} has a role in biofilm dispersion. This would involve testing ParP_{Pa} expression levels in dispersed cells, if deletion of ParP_{Pa} affects dispersion, c-di-GMP levels, and NicD and BldA localization, localization studies of both ParP_{Pa} and DipA in dispersed cells compared with planktonic cells, and determining which domains of DipA and ParP_{Pa} are required for their interaction. These experiments would show if ParP_{Pa} is expressed in dispersed cells along with DipA and if ParP_{Pa} is required for biofilm dispersion, modulation of c-di-GMP levels or NicD and BldA localization. The localization of ParP_{Pa} and DipA in dispersed and planktonic cells would show if

they are co-localized in these different growth phases. Overall, these results would allow for a definitive determination if ParP_{Pa} is linked to biofilm dispersion.

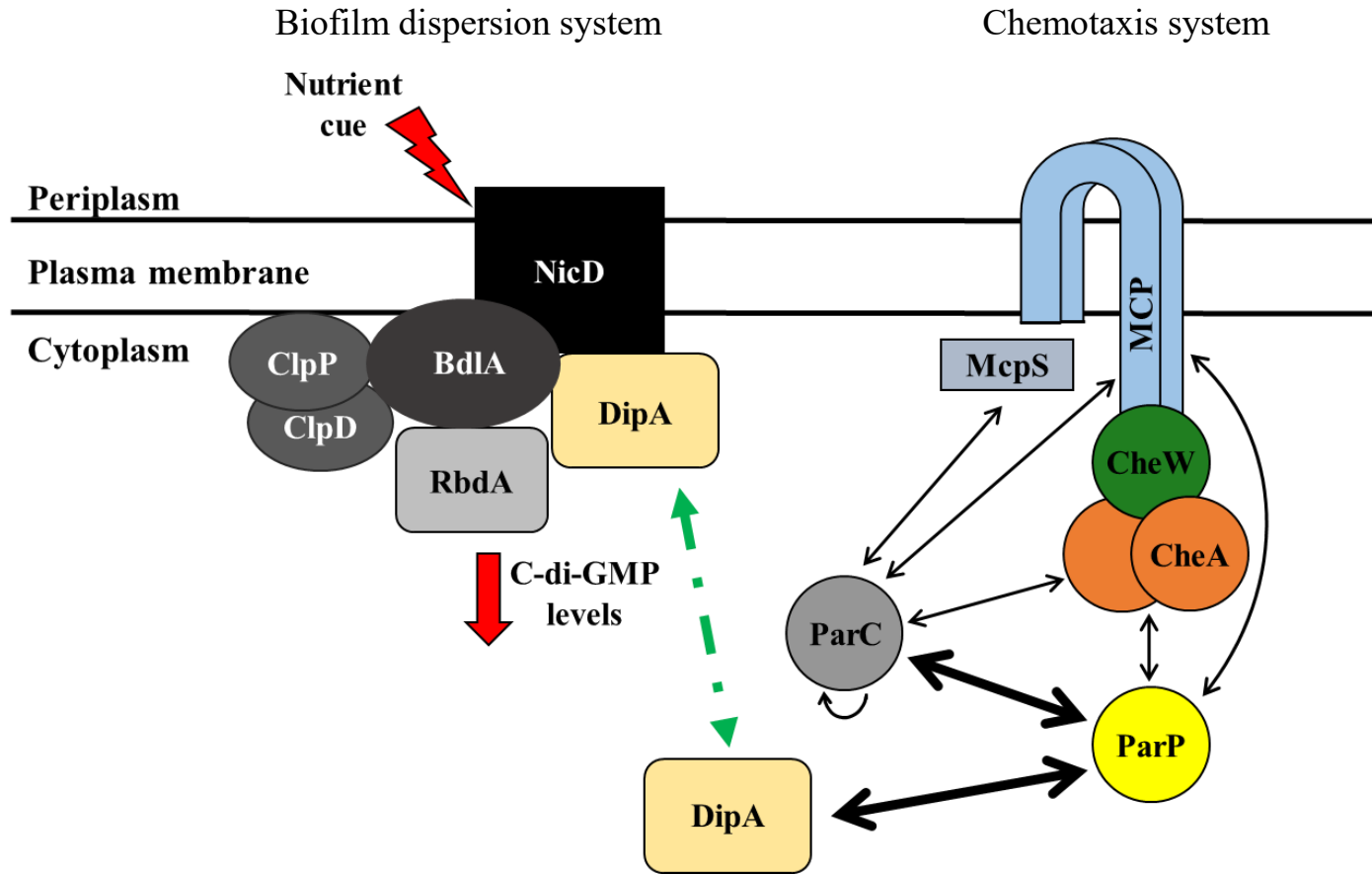


Figure 4.1 – Model showing B2H interactions linking the Par-like proteins with the chemotaxis and biofilm dispersion systems of *P. aeruginosa*. Black arrows indicate direct protein-protein interactions, with thicker arrows being a stronger interaction. The green dashed arrow points to the different roles that DipA has in regards to biofilm dispersion and chemotaxis. The red arrow pointing down indicates a decrease in c-di-GMP levels. The red lightning symbol represents a nutrient cue that is sensed by NicD.

REFERENCES

1. Sourjik V. 2004. Receptor clustering and signal processing in *E. coli* chemotaxis. Trends Microbiol 12:569-76.
2. Wadhams GH, Armitage JP. 2004. Making sense of it all: bacterial chemotaxis. Nat Rev Mol Cell Biol 5:1024-37.
3. Parkinson JS, Ames P, Studdert CA. 2005. Collaborative signaling by bacterial chemoreceptors. Curr Opin Microbiol 8:116-21.
4. Oku S, Komatsu A, Nakashimada Y, Tajima T, Kato J. 2014. Identification of *Pseudomonas fluorescens* chemotaxis sensory proteins for malate, succinate, and fumarate, and their involvement in root colonization. Microbes Environ 29:413-9.
5. Morgan DG, Baumgartner JW, Hazelbauer GL. 1993. Proteins antigenically related to methyl-accepting chemotaxis proteins of *Escherichia coli* detected in a wide range of bacterial species. J Bacteriol 175:133-40.
6. Ames P, Parkinson JS. 1988. Transmembrane signaling by bacterial chemoreceptors: *E. coli* transducers with locked signal output. Cell 55:817-26.
7. Roberts MA, Wadhams GH, Hadfield KA, Tickner S, Armitage JP. 2012. ParA-like protein uses nonspecific chromosomal DNA binding to partition protein complexes. Proc Natl Acad Sci U S A 109:6698-703.
8. Chandrashekhar K, Kassem II, Rajashekara G. 2017. *Campylobacter jejuni* transducer like proteins: Chemotaxis and Beyond. Gut Microbes:1-12.
9. Surette MG, Levit M, Liu Y, Lukat G, Ninfa EG, Ninfa A, Stock JB. 1996. Dimerization is required for the activity of the protein histidine kinase CheA that mediates signal transduction in bacterial chemotaxis. J Biol Chem 271:939-45.
10. Hazelbauer GL, Lai WC. 2010. Bacterial chemoreceptors: providing enhanced features to two-component signaling. Curr Opin Microbiol 13:124-32.
11. Briegel A, Wong ML, Hodges HL, Oikonomou CM, Piasta KN, Harris MJ, Fowler DJ, Thompson LK, Falke JJ, Kiessling LL, Jensen GJ. 2014. New insights into bacterial chemoreceptor array structure and assembly from electron cryotomography. Biochemistry 53:1575-85.
12. Parkinson JS, Hazelbauer GL, Falke JJ. 2015. Signaling and sensory adaptation in *Escherichia coli* chemoreceptors: 2015 update. Trends Microbiol 23:257-66.
13. Park H, Im W, Seok C. 2011. Transmembrane signaling of chemotaxis receptor Tar: insights from molecular dynamics simulation studies. Biophys J 100:2955-63.

14. Barnakov AN, Barnakova LA, Hazelbauer GL. 1998. Comparison in vitro of a high- and a low-abundance chemoreceptor of *Escherichia coli*: similar kinase activation but different methyl-accepting activities. *J Bacteriol* 180:6713-8.
15. Ames P, Zhou Q, Parkinson JS. 2014. HAMP domain structural determinants for signalling and sensory adaptation in Tsr, the *Escherichia coli* serine chemoreceptor. *Mol Microbiol* 91:875-86.
16. Kitanovic S, Ames P, Parkinson JS. 2011. Mutational analysis of the control cable that mediates transmembrane signaling in the *Escherichia coli* serine chemoreceptor. *J Bacteriol* 193:5062-72.
17. Coleman MD, Bass RB, Mehan RS, Falke JJ. 2005. Conserved glycine residues in the cytoplasmic domain of the aspartate receptor play essential roles in kinase coupling and on-off switching. *Biochemistry* 44:7687-95.
18. Alexander RP, Zhulin IB. 2007. Evolutionary genomics reveals conserved structural determinants of signaling and adaptation in microbial chemoreceptors. *Proc Natl Acad Sci U S A* 104:2885-90.
19. Othmer HG, Xin X, Xue C. 2013. Excitation and adaptation in bacteria—a model signal transduction system that controls taxis and spatial pattern formation. *Int J Mol Sci* 14:9205-48.
20. Wu J, Li J, Li G, Long DG, Weis RM. 1996. The receptor binding site for the methyltransferase of bacterial chemotaxis is distinct from the sites of methylation. *Biochemistry* 35:4984-93.
21. Barnakov AN, Barnakova LA, Hazelbauer GL. 1999. Efficient adaptational demethylation of chemoreceptors requires the same enzyme-docking site as efficient methylation. *Proc Natl Acad Sci U S A* 96:10667-72.
22. Jahreis K, Morrison TB, Garzón A, Parkinson JS. 2004. Chemotactic signaling by an *Escherichia coli* CheA mutant that lacks the binding domain for phosphoacceptor partners. *J Bacteriol* 186:2664-72.
23. Surette MG, Stock JB. 1996. Role of alpha-helical coiled-coil interactions in receptor dimerization, signaling, and adaptation during bacterial chemotaxis. *J Biol Chem* 271:17966-73.
24. Nishiyama S, Garzón A, Parkinson JS. 2014. Mutational analysis of the P1 phosphorylation domain in *Escherichia coli* CheA, the signaling kinase for chemotaxis. *J Bacteriol* 196:257-64.

25. Bourret RB, Davagnino J, Simon MI. 1993. The carboxy-terminal portion of the CheA kinase mediates regulation of autophosphorylation by transducer and CheW. *J Bacteriol* 175:2097-101.
26. Levit MN, Liu Y, Stock JB. 1999. Mechanism of CheA protein kinase activation in receptor signaling complexes. *Biochemistry* 38:6651-8.
27. Szurmant H, Ordal GW. 2004. Diversity in chemotaxis mechanisms among the bacteria and archaea. *Microbiol Mol Biol Rev* 68:301-19.
28. Hess JF, Bourret RB, Simon MI. 1988. Histidine phosphorylation and phosphoryl group transfer in bacterial chemotaxis. *Nature* 336:139-43.
29. Sarkar MK, Paul K, Blair D. 2010. Chemotaxis signaling protein CheY binds to the rotor protein FliN to control the direction of flagellar rotation in *Escherichia coli*. *Proc Natl Acad Sci U S A* 107:9370-5.
30. Bourret RB, Hess JF, Simon MI. 1990. Conserved aspartate residues and phosphorylation in signal transduction by the chemotaxis protein CheY. *Proc Natl Acad Sci U S A* 87:41-5.
31. Sim M, Koirala S, Picton D, Strahl H, Hoskisson PA, Rao CV, Gillespie CS, Aldridge PD. 2017. Growth rate control of flagellar assembly in *Escherichia coli* strain RP437. *Sci Rep* 7:41189.
32. Sircar R, Borbat PP, Lynch MJ, Bhatnagar J, Beyersdorf MS, Halkides CJ, Freed JH, Crane BR. 2015. Assembly states of FliM and FliG within the flagellar switch complex. *J Mol Biol* 427:867-86.
33. Kim M, Bird JC, Van Parys AJ, Breuer KS, Powers TR. 2003. A macroscopic scale model of bacterial flagellar bundling. *Proc Natl Acad Sci U S A* 100:15481-5.
34. Silversmith RE, Guanga GP, Betts L, Chu C, Zhao R, Bourret RB. 2003. CheZ-mediated dephosphorylation of the *Escherichia coli* chemotaxis response regulator CheY: role for CheY glutamate 89. *J Bacteriol* 185:1495-502.
35. Porter SL, Wadhams GH, Armitage JP. 2011. Signal processing in complex chemotaxis pathways. *Nat Rev Microbiol* 9:153-65.
36. Kentner D, Sourjik V. 2009. Dynamic map of protein interactions in the *Escherichia coli* chemotaxis pathway. *Mol Syst Biol* 5:238.
37. Saxl RL, Anand GS, Stock AM. 2001. Synthesis and biochemical characterization of a phosphorylated analogue of the response regulator CheB. *Biochemistry* 40:12896-903.

38. Kehry MR, Doak TG, Dahlquist FW. 1985. Sensory adaptation in bacterial chemotaxis: regulation of demethylation. *J Bacteriol* 163:983-90.
39. Levin MD, Shimizu TS, Bray D. 2002. Binding and diffusion of CheR molecules within a cluster of membrane receptors. *Biophys J* 82:1809-17.
40. Segall JE, Block SM, Berg HC. 1986. Temporal comparisons in bacterial chemotaxis. *Proc Natl Acad Sci U S A* 83:8987-91.
41. Cardozo MJ, Massazza DA, Parkinson JS, Studdert CA. 2010. Disruption of chemoreceptor signalling arrays by high levels of CheW, the receptor-kinase coupling protein. *Mol Microbiol* 75:1171-81.
42. Sourjik V, Armitage JP. 2010. Spatial organization in bacterial chemotaxis. *EMBO J* 29:2724-33.
43. Cannistraro VJ, Glekas GD, Rao CV, Ordal GW. 2011. Cellular stoichiometry of the chemotaxis proteins in *Bacillus subtilis*. *J Bacteriol* 193:3220-7.
44. Slovak PM, Wadhams GH, Armitage JP. 2005. Localization of MreB in *Rhodobacter sphaeroides* under conditions causing changes in cell shape and membrane structure. *J Bacteriol* 187:54-64.
45. Wadhams GH, Warren AV, Martin AC, Armitage JP. 2003. Targeting of two signal transduction pathways to different regions of the bacterial cell. *Mol Microbiol* 50:763-70.
46. Chiu SW, Roberts MA, Leake MC, Armitage JP. 2013. Positioning of chemosensory proteins and FtsZ through the *Rhodobacter sphaeroides* cell cycle. *Mol Microbiol* 90:322-37.
47. Jones CW, Armitage JP. 2015. Positioning of bacterial chemoreceptors. *Trends Microbiol* 23:247-56.
48. Ringgaard S, Schirner K, Davis BM, Waldor MK. 2011. A family of ParA-like ATPases promotes cell pole maturation by facilitating polar localization of chemotaxis proteins. *Genes Dev* 25:1544-55.
49. Briegel A, Ortega DR, Mann P, Kjær A, Ringgaard S, Jensen GJ. 2016. Chemotaxis cluster 1 proteins form cytoplasmic arrays in *Vibrio cholerae* and are stabilized by a double signaling domain receptor DosM. *Proc Natl Acad Sci U S A* 113:10412-7.
50. Ringgaard S, Hubbard T, Mandlik A, Davis BM, Waldor MK. 2015. RpoS and quorum sensing control expression and polar localization of *Vibrio cholerae* chemotaxis cluster III proteins in vitro and in vivo. *Mol Microbiol* 97:660-75.

51. Ringgaard S, Zepeda-Rivera M, Wu X, Schirner K, Davis BM, Waldor MK. 2014. ParP prevents dissociation of CheA from chemotactic signaling arrays and tethers them to a polar anchor. *Proc Natl Acad Sci U S A* 111:E255-64.
52. Maddock JR, Shapiro L. 1993. Polar location of the chemoreceptor complex in the *Escherichia coli* cell. *Science* 259:1717-23.
53. Greenfield D, McEvoy AL, Shroff H, Crooks GE, Wingreen NS, Betzig E, Liphardt J. 2009. Self-organization of the *Escherichia coli* chemotaxis network imaged with super-resolution light microscopy. *PLoS Biol* 7:e1000137.
54. Iniesta AA. 2014. ParABS system in chromosome partitioning in the bacterium *Myxococcus xanthus*. *PLoS One* 9:e86897.
55. Gerdes K, Howard M, Szardenings F. 2010. Pushing and pulling in prokaryotic DNA segregation. *Cell* 141:927-42.
56. Hester CM, Lutkenhaus J. 2007. Soj (ParA) DNA binding is mediated by conserved arginines and is essential for plasmid segregation. *Proc Natl Acad Sci U S A* 104:20326-31.
57. Million-Weaver S, Camps M. 2014. Mechanisms of plasmid segregation: have multicopy plasmids been overlooked? *Plasmid* 75:27-36.
58. Donovan C, Schwaiger A, Krämer R, Bramkamp M. 2010. Subcellular localization and characterization of the ParAB system from *Corynebacterium glutamicum*. *J Bacteriol* 192:3441-51.
59. Adams DW, Wu LJ, Errington J. 2014. Cell cycle regulation by the bacterial nucleoid. *Curr Opin Microbiol* 22:94-101.
60. Lutkenhaus J. 2012. The ParA/MinD family puts things in their place. *Trends Microbiol* 20:411-8.
61. Yamaichi Y, Bruckner R, Ringgaard S, Möll A, Cameron DE, Briegel A, Jensen GJ, Davis BM, Waldor MK. 2012. A multidomain hub anchors the chromosome segregation and chemotactic machinery to the bacterial pole. *Genes Dev* 26:2348-60.
62. Wadhams GH, Martin AC, Warren AV, Armitage JP. 2005. Requirements for chemotaxis protein localization in *Rhodobacter sphaeroides*. *Mol Microbiol* 58:895-902.
63. Porter SL, Warren AV, Martin AC, Armitage JP. 2002. The third chemotaxis locus of *Rhodobacter sphaeroides* is essential for chemotaxis. *Mol Microbiol* 46:1081-94.
64. Kearns DB. 2010. A field guide to bacterial swarming motility. *Nat Rev Microbiol* 8:634-44.

65. Diaz MH, Hauser AR. 2010. *Pseudomonas aeruginosa* cytotoxin ExoU is injected into phagocytic cells during acute pneumonia. *Infect Immun* 78:1447-56.
66. Fulcher NB, Holliday PM, Klem E, Cann MJ, Wolfgang MC. 2010. The *Pseudomonas aeruginosa* Chp chemosensory system regulates intracellular cAMP levels by modulating adenylate cyclase activity. *Mol Microbiol* 76:889-904.
67. Hauser AR, Jain M, Bar-Meir M, McColley SA. 2011. Clinical significance of microbial infection and adaptation in cystic fibrosis. *Clin Microbiol Rev* 24:29-70.
68. Strateva T, Yordanov D. 2009. *Pseudomonas aeruginosa* - a phenomenon of bacterial resistance. *J Med Microbiol* 58:1133-48.
69. Taylor PK, Yeung AT, Hancock RE. 2014. Antibiotic resistance in *Pseudomonas aeruginosa* biofilms: towards the development of novel anti-biofilm therapies. *J Biotechnol* 191:121-30.
70. Alvarez-Ortega C, Harwood CS. 2007. Identification of a malate chemoreceptor in *Pseudomonas aeruginosa* by screening for chemotaxis defects in an energy taxis-deficient mutant. *Appl Environ Microbiol* 73:7793-5.
71. Sampedro I, Parales RE, Krell T, Hill JE. 2015. *Pseudomonas* chemotaxis. *FEMS Microbiol Rev* 39:17-46.
72. Kato J, Kim HE, Takiguchi N, Kuroda A, Ohtake H. 2008. *Pseudomonas aeruginosa* as a model microorganism for investigation of chemotactic behaviors in ecosystem. *J Biosci Bioeng* 106:1-7.
73. Masduki A, Nakamura J, Ohga T, Umezaki R, Kato J, Ohtake H. 1995. Isolation and characterization of chemotaxis mutants and genes of *Pseudomonas aeruginosa*. *J Bacteriol* 177:948-52.
74. Kato J, Nakamura T, Kuroda A, Ohtake H. 1999. Cloning and characterization of chemotaxis genes in *Pseudomonas aeruginosa*. *Biosci Biotechnol Biochem* 63:155-61.
75. Ferrández A, Hawkins AC, Summerfield DT, Harwood CS. 2002. Cluster II che genes from *Pseudomonas aeruginosa* are required for an optimal chemotactic response. *J Bacteriol* 184:4374-83.
76. O'Connor JR, Kuwada NJ, Huangyutitham V, Wiggins PA, Harwood CS. 2012. Surface sensing and lateral subcellular localization of WspA, the receptor in a chemosensory-like system leading to c-di-GMP production. *Mol Microbiol* 86:720-9.

77. Güvener ZT, Tifrea DF, Harwood CS. 2006. Two different *Pseudomonas aeruginosa* chemosensory signal transduction complexes localize to cell poles and form and remould in stationary phase. *Mol Microbiol* 61:106-18.
78. Bardy SL, Maddock JR. 2005. Polar localization of a soluble methyl-accepting protein of *Pseudomonas aeruginosa*. *J Bacteriol* 187:7840-4.
79. Güvener ZT, Harwood CS. 2007. Subcellular location characteristics of the *Pseudomonas aeruginosa* GGDEF protein, WspR, indicate that it produces cyclic-di-GMP in response to growth on surfaces. *Mol Microbiol* 66:1459-73.
80. Ortega DR, Zhulin IB. 2016. Evolutionary Genomics Suggests That CheV Is an Additional Adaptor for Accommodating Specific Chemoreceptors within the Chemotaxis Signaling Complex. *PLoS Comput Biol* 12:e1004723.
81. Collins KD, Andermann TM, Draper J, Sanders L, Williams SM, Araghi C, Ottemann KM. 2016. The *Helicobacter pylori* CZB Cytoplasmic Chemoreceptor TlpD Forms an Autonomous Polar Chemotaxis Signaling Complex That Mediates a Tactic Response to Oxidative Stress. *J Bacteriol* 198:1563-75.
82. Morimoto YV, Nakamura S, Kami-ike N, Namba K, Minamino T. 2010. Charged residues in the cytoplasmic loop of MotA are required for stator assembly into the bacterial flagellar motor. *Mol Microbiol* 78:1117-29.
83. Cowles KN, Moser TS, Siryaporn A, Nyakudarika N, Dixon W, Turner JJ, Gitai Z. 2013. The putative Poc complex controls two distinct *Pseudomonas aeruginosa* polar motility mechanisms. *Mol Microbiol* 90:923-38.
84. Kulasekara BR, Kamischke C, Kulasekara HD, Christen M, Wiggins PA, Miller SI. 2013. c-di-GMP heterogeneity is generated by the chemotaxis machinery to regulate flagellar motility. *Elife* 2:e01402.
85. Pandza S, Baetens M, Park CH, Au T, Keyhan M, Martin A. 2000. The G-protein FlhF has a role in polar flagellar placement and general stress response induction in *Pseudomonas putida*. *Mol Microbiol* 36:414-23.
86. Wehbi H, Portillo E, Harvey H, Shimkoff AE, Scheurwater EM, Howell PL, Burrows LL. 2011. The peptidoglycan-binding protein FimV promotes assembly of the *Pseudomonas aeruginosa* type IV pilus secretin. *J Bacteriol* 193:540-50.
87. Römling U, Galperin MY, Gomelsky M. 2013. Cyclic di-GMP: the first 25 years of a universal bacterial second messenger. *Microbiol Mol Biol Rev* 77:1-52.
88. Ross P, Weinhouse H, Aloni Y, Michaeli D, Weinberger-Ohana P, Mayer R, Braun S, de Vroom E, van der Marel GA, van Boom JH, Benziman M. 1987. Regulation of cellulose synthesis in *Acetobacter xylinum* by cyclic diguanylic acid. *Nature* 325:279-81.

89. Dahlstrom KM, Giglio KM, Sondermann H, O'Toole GA. 2016. The Inhibitory Site of a Diguanylate Cyclase Is a Necessary Element for Interaction and Signaling with an Effector Protein. *J Bacteriol* 198:1595-603.
90. Aldridge P, Paul R, Goymer P, Rainey P, Jenal U. 2003. Role of the GGDEF regulator PleD in polar development of *Caulobacter crescentus*. *Mol Microbiol* 47:1695-708.
91. Ryan RP, Lucey J, O'Donovan K, McCarthy Y, Yang L, Tolker-Nielsen T, Dow JM. 2009. HD-GYP domain proteins regulate biofilm formation and virulence in *Pseudomonas aeruginosa*. *Environ Microbiol* 11:1126-36.
92. Christen M, Kulasekara HD, Christen B, Kulasekara BR, Hoffman LR, Miller SI. 2010. Asymmetrical distribution of the second messenger c-di-GMP upon bacterial cell division. *Science* 328:1295-7.
93. Valentini M, Filloux A. 2016. Biofilms and Cyclic di-GMP (c-di-GMP) Signaling: Lessons from *Pseudomonas aeruginosa* and Other Bacteria. *J Biol Chem* 291:12547-55.
94. Chen Y, Liu S, Liu C, Huang Y, Chi K, Su T, Zhu D, Peng J, Xia Z, He J, Xu S, Hu W, Gu L. 2016. Dcsbis (PA2771) from *Pseudomonas aeruginosa* is a highly active diguanylate cyclase with unique activity regulation. *Sci Rep* 6:29499.
95. Basu Roy A, Sauer K. 2014. Diguanylate cyclase NicD-based signalling mechanism of nutrient-induced dispersion by *Pseudomonas aeruginosa*. *Mol Microbiol* 94:771-93.
96. Feirer N, Xu J, Allen KD, Koestler BJ, Bruger EL, Waters CM, White RH, Fuqua C. 2015. A Pterin-Dependent Signaling Pathway Regulates a Dual-Function Diguanylate Cyclase-Phosphodiesterase Controlling Surface Attachment in *Agrobacterium tumefaciens*. *MBio* 6:e00156.
97. Hay ID, Remminghorst U, Rehm BH. 2009. MucR, a novel membrane-associated regulator of alginate biosynthesis in *Pseudomonas aeruginosa*. *Appl Environ Microbiol* 75:1110-20.
98. Li Y, Heine S, Entian M, Sauer K, Frankenberg-Dinkel N. 2013. NO-induced biofilm dispersion in *Pseudomonas aeruginosa* is mediated by an MHYT domain-coupled phosphodiesterase. *J Bacteriol* 195:3531-42.
99. Ryjenkov DA, Simm R, Römling U, Gomelsky M. 2006. The PilZ domain is a receptor for the second messenger c-di-GMP: the PilZ domain protein YcgR controls motility in enterobacteria. *J Biol Chem* 281:30310-4.
100. Boehm A, Kaiser M, Li H, Spangler C, Kasper CA, Ackermann M, Kaefer V, Sourjik V, Roth V, Jenal U. 2010. Second messenger-mediated adjustment of bacterial swimming velocity. *Cell* 141:107-16.

101. Zorraquino V, García B, Latasa C, Echeverz M, Toledo-Arana A, Valle J, Lasa I, Solano C. 2013. Coordinated cyclic-di-GMP repression of *Salmonella* motility through YcgR and cellulose. *J Bacteriol* 195:417-28.
102. McCarter LL, Gomelsky M. 2015. Fifty ways to inhibit motility via cyclic di-GMP: the emerging *Pseudomonas aeruginosa* swarming story. *J Bacteriol* 197:406-9.
103. Kuchma SL, Delalez NJ, Filkins LM, Snavely EA, Armitage JP, O'Toole GA. 2015. Cyclic di-GMP-mediated repression of swarming motility by *Pseudomonas aeruginosa* PA14 requires the MotAB stator. *J Bacteriol* 197:420-30.
104. Suzuki T, Iino T. 1980. Isolation and characterization of multiflagellate mutants of *Pseudomonas aeruginosa*. *J Bacteriol* 143:1471-9.
105. Li Y, Xia H, Bai F, Xu H, Yang L, Yao H, Zhang L, Zhang X, Bai Y, Saris PE, Tolker-Nielsen T, Qiao M. 2007. Identification of a new gene PA5017 involved in flagella-mediated motility, chemotaxis and biofilm formation in *Pseudomonas aeruginosa*. *FEMS Microbiol Lett* 272:188-95.
106. Flemming HC, Wingender J. 2010. The biofilm matrix. *Nat Rev Microbiol* 8:623-33.
107. Guttenplan SB, Kearns DB. 2013. Regulation of flagellar motility during biofilm formation. *FEMS Microbiol Rev* 37:849-71.
108. Morgan R, Kohn S, Hwang SH, Hassett DJ, Sauer K. 2006. BdlA, a chemotaxis regulator essential for biofilm dispersion in *Pseudomonas aeruginosa*. *J Bacteriol* 188:7335-43.
109. Sauer K, Camper AK, Ehrlich GD, Costerton JW, Davies DG. 2002. *Pseudomonas aeruginosa* displays multiple phenotypes during development as a biofilm. *J Bacteriol* 184:1140-54.
110. Sauer K, Cullen MC, Rickard AH, Zeef LA, Davies DG, Gilbert P. 2004. Characterization of nutrient-induced dispersion in *Pseudomonas aeruginosa* PAO1 biofilm. *J Bacteriol* 186:7312-26.
111. Roy AB, Petrova OE, Sauer K. 2012. The phosphodiesterase DipA (PA5017) is essential for *Pseudomonas aeruginosa* biofilm dispersion. *J Bacteriol* 194:2904-15.
112. Petrova OE, Sauer K. 2012. PAS domain residues and prosthetic group involved in BdlA-dependent dispersion response by *Pseudomonas aeruginosa* biofilms. *J Bacteriol* 194:5817-28.
113. Newman JR, Fuqua C. 1999. Broad-host-range expression vectors that carry the L-arabinose-inducible *Escherichia coli* araBAD promoter and the araC regulator. *Gene* 227:197-203.

114. Simon R, Prierer U, Puhler A. 1983. A broad host range mobilization system for *in vivo* genetic engineering: Transposon mutagenesis in Gram negative bacteria., vol 1, p 784-791. Biotechnology.
115. Hoang TT, Karkhoff-Schweizer RR, Kutchma AJ, Schweizer HP. 1998. A broad-host-range Flp-FRT recombination system for site-specific excision of chromosomally-located DNA sequences: application for isolation of unmarked *Pseudomonas aeruginosa* mutants. *Gene* 212:77-86.
116. Horton RM, Cai ZL, Ho SN, Pease LR. 1990. Gene splicing by overlap extension: tailor-made genes using the polymerase chain reaction. *Biotechniques* 8:528-35.
117. Faguy DM, Bayley DP, Kostyukova AS, Thomas NA, Jarrell KF. 1996. Isolation and characterization of flagella and flagellin proteins from the Thermoacidophilic archaea *Thermoplasma volcanium* and *Sulfolobus shibatae*. *J Bacteriol* 178:902-5.
118. Jansari VH, Potharla VY, Riddell GT, Bardy SL. 2016. Twitching motility and cAMP levels: signal transduction through a single methyl-accepting chemotaxis protein. *FEMS Microbiol Lett* 363.
119. Sievers F, Wilm A, Dineen D, Gibson TJ, Karplus K, Li W, Lopez R, McWilliam H, Remmert M, Söding J, Thompson JD, Higgins DG. 2011. Fast, scalable generation of high-quality protein multiple sequence alignments using Clustal Omega. *Mol Syst Biol* 7:539.
120. Winsor GL, Griffiths EJ, Lo R, Dhillon BK, Shay JA, Brinkman FS. 2016. Enhanced annotations and features for comparing thousands of *Pseudomonas* genomes in the *Pseudomonas* genome database. *Nucleic Acids Res* 44:D646-53.
121. Dmowski M, Jagura-Burdzy G. 2011. Mapping of the interactions between partition proteins Delta and Omega of plasmid pSM19035 from *Streptococcus pyogenes*. *Microbiology* 157:1009-20.
122. Buensuceso RN, Nguyen Y, Zhang K, Daniel-Ivad M, Sugiman-Marangos SN, Fleetwood AD, Zhulin IB, Junop MS, Howell PL, Burrows LL. 2016. The Conserved Tetratricopeptide Repeat-Containing C-Terminal Domain of *Pseudomonas aeruginosa* FimV Is Required for Its Cyclic AMP-Dependent and -Independent Functions. *J Bacteriol* 198:2263-74.
123. Murray TS, Kazmierczak BI. 2006. FlhF is required for swimming and swarming in *Pseudomonas aeruginosa*. *J Bacteriol* 188:6995-7004.

CURRICULUM VITAE

Jesse Reinhardt

Place of birth: Chicago, IL

EDUCATION

Ph.D., University of Wisconsin – Milwaukee, May 2017

Major: Biological Sciences – Microbiology

Secondary area of concentration: Molecular Biology

B.S., Illinois Institute of Technology, December 2009

Major: Biochemistry

DISSERTATION TITLE: A Novel Link Between the Chemotaxis and Biofilm Dispersion Systems of *Pseudomonas aeruginosa*

AWARDS AND HONORS

2016 Ruth Walker Graduate Grant-in-Aid Award, Department of Biological Sciences

2011-2016 Chancellor's Graduate Student Award

2015 Graduate Student Travel Award

RESEARCH EXPERIENCE

University of Wisconsin-Milwaukee

2011-2017 Graduate Student Researcher

2015-2016 Undergraduate Research Mentor

Illinois Institute of Technology

2008-2009 Undergraduate Student Researcher

TEACHING EXPERIENCE

Graduate Teaching Assistant

2015-2017 General Microbiology (Bio Sci 383)

2011-2014 General Survey of Microbiology (Bio Sci 101)

MEMBERSHIPS, CLUBS AND ORGANIZATIONS

2014 American Society of Microbiology

2006-2007 Center for Science Success

2006-2007 Phi Theta Kappa - Honor Society of the Two-Year College

VOLUNTEER EXPERIENCE

Badger State Science and Engineering Fair
2016 Specialty Award Judge

2014-2015 Scientific Process Judge

Northwestern Lake Forest Hospital
2010 Registration Volunteer

North Branch Restoration Project
2005-2007 Natural Area Restoration Volunteer

CONFERENCES AND SYMPOSIUMS

Presentations

March 31, 2017 A novel link between the chemotaxis and biofilm dispersion systems of *Pseudomonas aeruginosa*, University of Wisconsin-Milwaukee Biological Sciences Colloquium. Milwaukee, WI.

April 22, 2016 A Par-like system involved in flagellar-based motility and chemotaxis protein complex stability in *Pseudomonas aeruginosa*. University of Wisconsin-Milwaukee Biological Sciences Research Symposium. Milwaukee, WI.

Posters

January 19-20, 2015 A partitioning-like system involved in flagellar-based motility in *Pseudomonas aeruginosa*. Bacterial Locomotion and Signal Transduction (BLAST) XIII. Tucson, AZ.

April 25, 2014 PA1462: A ParA-like protein involved in swimming motility in *Pseudomonas aeruginosa*. University of Wisconsin-Milwaukee Biological Sciences Research Symposium. Milwaukee, WI.

PUBLICATIONS

A Novel Link Between the Chemotaxis and Biofilm Dispersion Systems of *Pseudomonas aeruginosa*. Reinhardt, J. & Bardy, S. L. (in preparation)